Preprints.org

Article

Not peer-reviewed version

Peraluminous Rare Metal Granites in Iberia: Geochemical, Mineralogical, Geothermobarometric and Petrogenetic Constraints

Francisco Javier López-Moro *, Alejandro Díez-Montes, Susana Maria Timón Sánchez, Teresa Llorens González, Teresa Sánchez García

Posted Date: 3 January 2024

doi: 10.20944/preprints202401.0163.v1

Keywords: intensive variables; parental magma; exsolved fluid phase; albitization; Nb/Ta ratio; columbite group minerals; Iberian Massif

Preprints.org is a free multidiscipline platform providing preprint service that is dedicated to making early versions of research outputs permanently available and citable. Preprints posted at Preprints.org appear in Web of Science, Crossref, Google Scholar, Scilit, Europe PMC.

Copyright: This is an open access article distributed under the Creative Commons Attribution License which permits unrestricted use, distribution, and reproduction in any medium, provided the original work is properly cited.

Preprints (www.preprints.org) | NOT PEER-REVIEWED | Posted: 3 January 2024 doi:10.20944/preprints202401.0163.v1

Disclaimer/Publisher's Note: The statements, opinions, and data contained in all publications are solely those of the individual author(s) and contributor(s) and not of MDPI and/or the editor(s). MDPI and/or the editor(s) disclaim responsibility for any injury to people or property resulting from any ideas, methods, instructions, or products referred to in the content.

Article

Peraluminous Rare Metal Granites in Iberia: Geochemical, Mineralogical, Geothermobarometric and Petrogenetic Constraints

Francisco Javier López-Moro [1,*], Alejandro Díez Montes [1], Susana María Timón-Sánchez [1], Teresa Llorens González [1] and Teresa Sánchez-García [2]

[1] IGME-CSIC, Oficina de Salamanca, Plaza de la Constitución 1, 37001, Salamanca (Spain)
[2] IGME-CSIC, Ríos Rosas, 23, 28003, Madrid, Spain
* Correspondence: fj.lopez@igme.es

Abstract: The intensive variables, geochemical, mineralogical and petrogenetic constraints of the Iberian rare metal granites, many of them unknown, are presented. It allows to distinguish two main granitic types with contrasting characteristics: Nb-Ta-rich granites and Nb-Ta-poor granites. The former have lower emplacement temperatures, higher water contents and probably lower emplacement pressures than Nb-Ta-poor granites. Nb-Ta-rich granites also have higher fluoride contents, strong fractionation into twin pairs such as Zr-Hf, Y-Ho and Nb-Ta, and an abundant, probably exsolved, fluid phase, which is not or not as evident in Nb-Ta-poor granites, probably in part because the Nb-Ta-rich granites reach their solidus later (about 550 ºC). The geochemical signature of the Iberian rare metal granites follows the trends of mainly two-mica granites and P-rich cordierite granites, but also of granodiorites and even type I granites, suggesting that the rare metal granites may have different parental magmas. Thermodynamic modeling shows that many of the geochemical characteristics of the RMGs can be explained by a process of extreme differentiation, while others cannot, e.g. Na evolution. In terms of ore deposition, white mica plays a very important role in explaining the variation of the Ta/Nb ratio, although the latter could also be controlled by late Nb-Ta oxides crystallization and even by acidic fluids that remove Nb relative to Ta from earlier Nb-Ta oxides.

Keywords: intensive variables; parental magma; exsolved fluid phase; albitization; Nb/Ta ratio; columbite group minerals; Iberian Massif

1. Introduction

Recently, the European Union has funded research projects to determine the availability of critical metals in the European Union in the face of the challenge of ecological transition and the extensive use of electronic devices in our daily lives. ProMine, ORAMA, GeoERA, SCRREN, FutuRaM and GSEU are good examples of such projects (see European Geological Data Infrastructure https://www.europe-geology.eu/). Since the recycling processes of these metals do not cover more than a minimal part of the needs of the current industry, it is necessary to find or re-exploit mineral deposits that could contain these critical metals. Rare metal granites (RMGs) are good candidates. Although in many cases these granites do not have high grades of these metals, they do have high tonnages, and in addition, they usually have, at least to a large extent, alteration/weathering processes (kaolinization) that make their extraction and treatment in processing plants very easy and inexpensive, since they do not need to be crushed or even milled. Another advantage of the kaolinization process is that it can increase the concentration of the ore up to twofold by mass losses of the silicate fraction [1].

In Iberia, rare metal granites were discovered in the last century and were the subject of studies in the 70's and 80's by mining companies and research centers, in most cases paid by these companies, mainly benefiting Sn and W and exceptionally Ta. These studies resulted in mostly internal reports

© 2024 by the author(s). Distributed under a Creative Commons CC BY license.

Preprints (www.preprints.org) | NOT PEER-REVIEWED | Posted: 3 January 2024 doi:10.20944/preprints202401.0163.v1

that were difficult for the public to access and, in exceptional cases, this information was used for the realization of doctoral theses and for publication in local research articles. A dramatic drop in the price of these metals in the mid-1980s led to the closure of all mines associated with these granites in Iberia. After 30-40 years, the high market prices of elements such as Ta, Nb, Sn, W, Be, REE have encouraged mining companies to look for new deposits or to re-evaluate the viability of the rare metal granites mined in the 70's-80's in Iberia, as in the case of the rare metal granites of Penouta (Strategic Minerals Europe), El Trasquilón (Grabat Energy), Fuentes de Oñoro (SIEMCALSA, Berkeley), Golpejas (Solid Mines, Salamanca Ingenieros), Argemela (PANNN Consultores de Geociências Lda.) and the alkaline orthogneisses of Galiñeiro (Umbono Capital), generating more information [2–4]. In addition, European countries and the European Union have recently shown further interest in this type of deposit, funding research projects that have produced a great deal of information, both published [5,6] and unpublished.

This work gathers all the available structural, geochemical and chemical-mineralogical data generated by mining companies and research centers in the last 50 years, as well as the chemical-mineralogical data obtained in this work, to characterize the Iberian rare metal granites from a geochemical, mineralogical and geothermometric point of view, in order to distinguish the different rare metal granites in Iberia and to decipher the main factors that most control their peculiar geochemistry and the mineralization itself.

2. Geological Setting

The Iberian RMGs are located in the Variscan belt of Western Europe, which was formed by the convergence of two lithospheric plates: Gondwana to the south and Laurussia to the north [7] although other smaller blocks or terranes have been recognized. The early imprint of this collision was recorded by the development of active margins and arcs and the subsequent accretion of arc units onto continental blocks, triggering HP/HT eclogite units and the accretion of ophiolites formed in supra-subduction environments [8]. Nappe stacking also was developed, with thrusting propagating to the outer zones, while inner parts underwent partial melting in the lower crust and extensional detachment and thermal domes were formed (e.g., [9,10]). Late tectonic evolution developed syn-convergent extension in the internal domains, crustal-scale transcurret shear zones and intrusion of syn-kinematic magmatism [11–13].

Four major stages of magmatism associated with the Variscan orogeny have been distinguished [14]. A Middle/Late Devonian magmatism of calc-alkaline and tholeiitic affinity associated with a magmatic arc and a subduction zone. Oceanic rocks (alkaline and tholeiitic basalts and dolerites) are also formed during this stage. The second stage is Pre-Late Visean and corresponds to an aluminous magmatism with granites with cordierite and biotite formed by melting of the continental crust probably related to cortical thickening. The third corresponds to a late Visean magmatism with lava flows, ignimbrites and pyroclastic deposits, rhyolitic and dacitic dikes, hypovolcanic microgranites and red granites. Its origin seems to be related to heat input from the mantle, although a contribution from the mantle as a source is not ruled out. Another stage of magmatism occurred between the Namurian and the Westphanian, a very productive period, with the generation of peraluminous magmas (porphyritic granites and biotite-muscovite leucogranites) originating from the melting of the continental crust. The last stage corresponds to the Stephanian magmatism, related to lithospheric delamination processes at the end of the Variscan orogeny. In this stage migmatitic domes and cordieritic granites were formed. The magmatism of the RMGs is thought to be quite late (Westphalian-Stephanian), coeval with the Sn-W mineralization and also related to late extensional processes.

In the European Variscan Belt, RMGs occur either in the inner to outermost areas of the belt [15], extending from Iberia to the Bohemian Massif. They outcrop in the Armorican Massif of France (e.g., Tréguennec, see [16]), the French Massif Central (e.g., Blond Massif, Richemont, Montebras, Beauvoir and Chavance, see [17–19]), the Iberian Massif (Penouta, Argemela, see [2,3,5,20]), the Bohemian Massif (Podlesi, Cinovec/Zinnwald, see see [21,22]), and Cornwall (e.g., St. Austell granites and the Tregonning-Godolphin granite, see [23,24]).

Preprints (www.preprints.org) | NOT PEER-REVIEWED | Posted: 3 January 2024 doi:10.20944/preprints202401.0163.v1

The European Variscan RMGs of the inner zones show differences with respect to the outer zones in geochemical terms, being most of those of the inner zones (French and Portuguese granites) richer in P, Al, Li, Sn, Rb and in the Ta/Nb ratio, than those of the outer zones (Bohemian and Cornwall Massifs) [15]. These differences can be extended to the granitic typology, since the granites of the outer zones are typically of type A of [25], while those of the inner zones are peraluminous granites. The reasons for these geochemical differences are poorly understood, but differences in source or partial melting temperature may be involved.

The Iberian RMGs outcrop in the Central Iberian Zone (CIZ) and the Galicia-Trás-os-Montes Zone (GTMZ) (Figure 1A). The CIZ corresponds to Gondwanan zones with early Ordovician magmatism, whereas the GTMZ contains the parautochthonous and allochthonous terranes with ophiolites and high pressure rocks. Based on tectonostratigraphic criteria, the CIZ has been divided into the Ollo de Sapo Domain (OSD) and the Schist Greywacke Complex Domain (SGCD). In the former, Late Cambrian to Early Ordovician subvolcanic, volcanic and volcanic-sedimentary rocks crop out in northeast-trending recumbent folds [26]. The SGCD consists of a metasedimentary turbidite sequence exposed in upright folds [27]. The GTMZ is divided into the Schist Domain (SD) and the Allochthonous Complex Domain (ACD). The former consists of siliciclastic sediments and metavulcanic rocks, whereas the ACD contains ophiolitic materials together with a mixture of continental and island arc materials [28]. The Variscan orogeny generated most of the structures, internal deformation and metamorphism in the Iberian Massif. Different stages of deformation have been described. They are as follows. A D1 phase produced overturned to recumbent folds and has been dated between 359 Ma and 336 Ma ($^{40}Ar/^{39}Ar$; [29]). A D2 phase resulted in thrusting towards the external zones, while in the lower part extensional events triggered crustal anataxis and pervasive foliation. Thrusting was dated between 343 and 321 Ma [29] and migmatization between 325 and 311 Ma (U-Pb in monazites; [26,30]). The D3 phase resulted in upright folds, open-to-close folds and strike-slip shear zones. An age of 315-306 Ma constrains this deformation phase (e.g., [31–33]). Iberian rare-metal granites range from those deformed by D2, as in the Golpejas granite [34], to those with no evidence of deformation, as in the Penouta [2] and Logrosán [35] granites.

3. Occurrences of Rare Metal Granites in the Central Iberian Zone and Data Sources

In this paper we will focus on granites where rare metal ore is disseminated in highly developed apogranites or leucogranites located in the Central Iberian Zone and Galicia-Trás os Montes Zone, i.e. Group B1 as defined by [36]. Geological and mineralogical characteristics of economic and subeconomic occurrences of B1 granite are summarized in Table 1. Whole rock data used in this work were obtained from external sources (Table 1) and mineral analyses were obtained from external sources, except for minerals from the Golpejas granite analyzed in this work (Table 1).

We have distinguished two major groups of these granites because they have different geochemical and geothermometric characteristics, as will be seen below: Nb-Ta-poor granites and Nb-Ta-rich granites. The group of Nb-Ta-rich rare metal granites includes the Penouta (Sn-Ta-Nb±Be), Golpejas (Sn-Ta-Nb±Li), Argemela (Li-Sn-Ta-Nb), Villardeciervos (Sn-Nb-Ta), Fuentes de Oñoro (Li-Sn-Ta-Nb), and Tres Arroyos (W-Li-Nb-Ta) granites (Figure 1A). The group of Nb-Ta-poor granites includes the granites of El Trasquilón (Sn-Li±Nb±Ta), Fontao (W±Sn±Nb), Logrosán (Sn±Nb), Laza (Sn±Ta), Ponte Segade (W±Nb±Ta), Beariz (Sn±Nb±Ta), Acebo (Li-W±Nb), Torrecilla de los Ángeles (Sn-W±Li), Belvis de Monroy (Be±Li), Pedroso de Acim (W-Sn-Li±Nb±Ta), and Jálama (Li±Nb) (Figure 1A). In these granites, mainly Sn or W has been mined, while the beneficiation of Nb-Ta has been scarce and limited in the 80's to the Golpejas and Penouta granites, and currently to the Penouta granite. There is no evidence of Li mining in these granites. The most extensively mined rare metal granites due to their high grades and/or reserves are the albite granites of Penouta, Golpejas and the granites of Fontao and El Trasquilón. A brief description of the most important Iberian RMGs is shown below.

Preprints (www.preprints.org) | NOT PEER-REVIEWED | Posted: 3 January 2024 doi:10.20944/preprints202401.0163.v1

Table 1. Iberian RMGs' outstanding characteristics and source of data.

Occurrence	Granite type	Mineralization	Maximum ore content (ppm)	Reserves (Mt)	Whole rock source	Mineral chemistry source
Penouta	AG/LP/NbTa-rich	Sn-Ta-Nb±Be	Sn: 3800; Ta: 226	>10	[2,37]	[3,4,38]
Golpejas	AG/HP/NbTa-rich	Sn-Ta-Nb±Li	Sn: 2097; Ta: 215	5-10	[38,39]	This work
Argemela	AG/HP/NbTa-rich	Li-Sn-Ta-Nb	Sn: 1960; Ta: 161	Unknown	[5,20,40]	[5,20]
Villardeciervos	AG/NbTa-rich	Sn-Nb-Ta	Sn: 439; Ta: 273	1-5	[41,42]	-
Fuentes de Oñoro	AG/MP/NbTa-rich	Li-Sn-Ta-Nb	Sn: 500*; Ta: 50*	<1	[43]	-
Tres Arroyos	LG/MP/NbTa-rich	W-Li-Nb-Ta	Sn: 781; Ta: 124	<1	[44,45]	[44]
El Trasquilón	AG/HP/NbTa-poor	Sn-Li±Nb±Ta	Sn: 5830; Ta: 78	1-5	[38,44,46]	[44]
Fontao	2M/MP/NbTa-poor	W±Sn±Nb	W: 266; Ta: 13	1-5	[38]	-
Logrosán	LG/MP/NbTa-poor	Sn±Nb	Sn: 1000; Ta: 5.7	<1	[35,47]	[35,47]
Laza	LG/NbTa-poor	Sn±Ta	Sn: 2300; Ta: 10	5-10	[48]	-
Ponte Segade	AG/MP/NbTa-poor	W±Nb±Ta	Sn: 110; Ta: 7	<1	[49]	[49]
Beariz	LG/MP/NbTa-poor	Sn±Nb±Ta	Sn: 105; Ta: 45	<1	[50]	[50]
Acebo	2M/NbTa-poor	Li-W±Nb	Sn: 60; Ta: 40	1-5	[51]	-
Torrecilla	2M/NbTa-poor	Sn-W±Li	Sn: 7200; Ta: -	1-5	[51]	-
Belvis de Monroy	LG/MP/NbTa-poor	Be±Li	Sn: 50; Ta: 5	Unknown	[52]	-
Pedroso de Acim	2M/MP/NbTa-poor	W-Sn-Li±Nb±Ta	Sn: 602; Ta: 29	<1	[44,51,53]	-
Jálama	2M/MP/NbTa-poor	Li±Nb	Sn: 44; Ta: 7	Unknown	[54]	-

AG: albite granite; LG: leucogranite; 2M: two-mica granite; LP: low-phosphorus granite; HP: high-phosphorus granite; MP: medium-phosphorus granite; LP: low-phosphorus granite; reserves from [36]; *: determined by portable XRF analyzer in this work; -: Not reported or referenced.

Preprints (www.preprints.org) | NOT PEER-REVIEWED | Posted: 3 January 2024 doi:10.20944/preprints202401.0163.v1

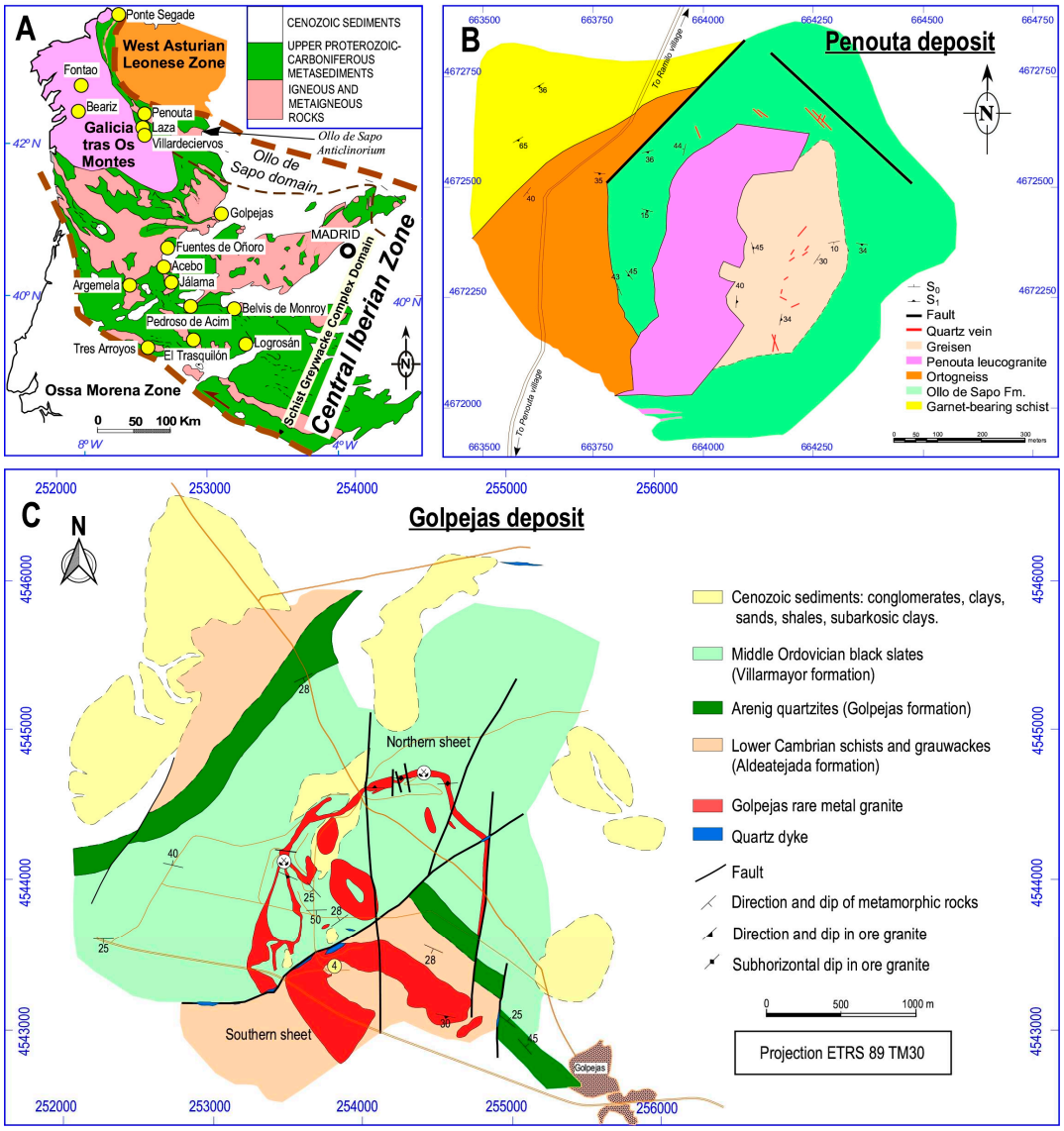

Figure 1. A) Location of Iberian rare metal granites in the Central Iberian Zone and Galicia-Trás os Montes Zone (Spain and Portugal). B) Geological map of the Penouta deposit (modified of [2]). C) Geological map of the Golpejas deposit (modified of [55]).

3.1. The Penouta Sn-Ta-Nb±Be Albite Granite

The Penouta granite outcrops in an area of about 0.2 km² and in its present state (strongly influenced by the old mining activities) it is elongated in a north-south direction (Figure 1B). This granite is a lenticular body, emplaced in the hinge of a D3 Variscan antiform [26,56], following the planar anisotropies of the wall rocks, mainly the orthogneiss Ollo de Sapo Fm and the paragneiss of the Viana do Bolo Serie [2]. Two main granitic facies can be distinguished: A fine-grained muscovite-rich granite at the base of the body with Sn-Nb-Ta ore and significant Be contents, and a fine-grained albite-rich granite at the apical zone of the body where the ore grade is higher. The mineralization consists mainly of magmatic disseminated cassiterite and columbite group minerals with values up to 226 ppm Ta, 89 ppm Nb and up to 0.38% Sn (Table 2). Flat-lying sheets of aplo-pegmatite can be found in the Penouta granite, especially in the apical zone. These structures are nearly horizontal tabular bodies, centimeters to meters thick, composed of different proportions of the main constituents (e.g., quartz-mica layers, albite layers, and quartz layers) rhythmically sandwiched. This granite developed, especially in the eastern zone, a Sn-enriched greisen (without Nb-Ta ore) in overlying metamorphic rocks. Mineralogically, the granite consists of quartz, albite, potassium

Preprints (www.preprints.org) | NOT PEER-REVIEWED | Posted: 3 January 2024 doi:10.20944/preprints202401.0163.v1

feldspar and white mica as major minerals, and garnet, beryl, zircon, apatite, monazite, fluorite, cassiterite and Nb-Ta oxides as accessory minerals [2–4]. Kaolinite is a secondary mineral mainly developed in the weathered leucogranite and its occurrence favored the mining of the deposit in the 80's.

Table 2. Whole-rock data and thermometric results of representative Iberian RMG's.

Granite	Golpejas			Penouta			Argemela			El Trasquilón			Logrosán		
Value	Max	Av	Std	Max	Av	Std	Max	Av	Std	Max	Av	Std	Max	Av	Std
SiO_2		69.6			74.2								74.0		
(wt.%)	74	6	3.39	77.20	6	1.45	74.41	69.69	5.26	76.60	71.22	2.15	3	70.52	6.22
TiO_2	0.05	0.05	0.00	0.01	0.00	0.00	0.07	0.05	0.27	0.09	0.05	0.01	0.33	0.19	0.06
		16.3			15.7								31.6		
Al_2O_3	24.2	0	2.19	18.20	1	0.66	21.02	17.31	3.57	21.10	17.00	1.63	1	16.49	4.25
FeOt	0.57	0.31	0.11	1.02	0.49	0.22	0.57	0.28	0.12	1.91	0.89	0.25	2.18	1.30	0.38
MnO	0.16	0.07	0.06	0.20	0.05	0.05	0.06	0.03	0.02	0.49	0.06	0.07	0.04	0.02	0.01
MgO	0.16	0.11	0.04	0.09	0.03	0.01	0.04	0.03	0.17	0.31	0.20	0.06	0.75	0.31	0.14
CaO	3.39	1.63	1.35	0.19	0.14	0.02	1.71	0.23	0.36	1.52	0.59	0.37	0.69	0.42	0.15
Na_2O	6.94	5.07	0.82	7.74	6.10	0.90	9.30	5.46	2.02	4.59	3.23	0.97	4.28	3.10	0.66
K_2O	4.16	3.14	0.61	4.07	3.30	0.36	5.16	2.56	1.12	5.37	3.37	0.65	8.50	4.87	1.03
P_2O_5	2.63	1.32	0.98	0.07	0.05	0.01	2.69	1.71	0.85	2.59	1.08	0.43	0.78	0.51	0.15
LOI	2.14	1.55	0.44	-	-	-	4.49	1.65	0.74	3.20	2.03	0.44	5.86	1.96	1.55
		100.			100.								99.9		
Total	100.4	3	0.15	102	2	1.01	100.3	98.9	0.68	101.1	99.75	0.86	9	98.6	0.87
A/CNK	1.55	1.13	0.19	1.83	1.14	0.11	2.01	1.56	1.04	2.26	1.84	1.01	2.73	1.49	0.37
A/NK	1.58	1.39	0.12	1.87	1.16	0.11	2.16	1.61	1.04	2.46	2.06	1.12	2.76	1.59	0.35
	1574														
F (ppm)	9	3249	3630	-	-	-	12500	4875	3287	5800	2457	1582	5495	1002	1534
Li	1084	86	98	129	129	-	5532	1607	1634	4555	318	413	780	132	209
Rb	2184	1030	282	1105	892	114	2448	1224	613	985	792	87	918	363	156
		27.8			34.9										66.5
Cs	97	2	20.39	56.00	8	7.02	350	89.97	99.86	81.00	81.00	-	275	70.32	5
		45.1		141.5	17.4	26.1									51.7
Ba	145	0	42.95	0	3	8	53	9.61	11.16	19.00	9.14	6.07	290	200	2
		86.4	204.8		17.3	14.0							77.0		13.4
Sr	875	1	8	62.60	8	0	677	42.83	113.3	90.00	37.09	24.70	0	44.50	7
													40.0		12.4
Pb	18	6.03	4.51	-	-	-	34.50	9.68	10.12	8.00	6.43	1.40	0	19.81	2
Cr	67	7.21	18.06	10.00	4.91	5.05	5.20	1.39	1.67	-	-	-	-	-	-
		12.5											20.0		
Ni	43	8	11.80	-	-	-	8.31	0.80	1.82	16.00	6.29	5.99	0	16.25	8.06
													21.0		
V	77	5.84	19.65	-	-	-	0.00	0.00	0.00	-	-	-	0	9.59	4.37
		17.2											50.0		11.8
Cu	75.5	7	22.02	-	-	-	36.64	8.71	9.32	-	-	-	0	12.50	3

Preprints (www.preprints.org) | NOT PEER-REVIEWED | Posted: 3 January 2024 doi:10.20944/preprints202401.0163.v1

Zn	139	64.2 2	23.19	0.72	0.28	0.13	134.0	45.53	39.79	116.0	89.57	20.74	100	44.24	30.8 8
As	24.3	6.84	6.36	-	-	-	103.9	13.63	29.10	266.0	95.00	84.22	1470	170.5 0	354. 6
Sc	-	-	-	-	-	-	0.22	0.01	0.04	-	-	-	6.00	2.44	1.71
Sn	2097	296	359.4	3800	521	449. 4	1960	686	453.2	5830	257	653	1000	114	242. 0
Nb	230	115	32.1	89	68	9.1	91	50	21.1	97	35	12.5	21.3	13	3.9
Ta	215	105	32.1	226	73	38.5	161	62	36.8	78.5	13	11.9	5.7	3	1.1
W	17.4	5.96	5.37	5.00	2.51	0.72	58.80	7.39	9.63	-	-	-	376	95.68	119. 4
Zr	39	29.6 7	5.09	31.00	20.2 1	4.52	28.60	13.64	4.10	139	59.67	22.25	118	74.00	19.7 8
Hf	7.83	5.41	1.21	8.50	6.87	0.87	5.36	2.73	1.05	6.21	2.91	0.78	3.10	2.29	0.56
Th	20	2.13	4.83	3.77	2.67	0.35	1.45	0.40	0.30	2.10	0.50	0.74	19.9 0	8.08	4.15
U	37.9	8.65	10.15	15.80	10.6 2	2.66	39.00	8.36	5.87	50.00	34.00	13.01	15.5 0	9.29	2.50
Ga	329	37.3 1	26.37	44.70	35.5 0	2.84	68.00	33.51	11.30	53.00	41.14	6.41	91.0 0	27.81	17.4 4
Be	103	44.7 6	33.41	125	125	-	385	95.44	84.30	-	-	-	23.0 0	11.00	6.95
Ge	8.46	4.05	1.58	-	-	-	5.54	2.13	2.31	-	-	-	3.80	1.98	1.14
Y	9.07	0.90	2.28	9.80	3.34	1.43	1.35	0.18	0.23	20.50	8.52	3.06	13.1 0	6.66	2.34
La	0.41	0.16	0.13	1.80	0.74	0.31	0.61	0.17	0.16	9.98	3.95	1.58	21.8 0	13.13	4.19
Ce	0.82	0.30	0.26	4.70	1.94	0.83	3.30	0.28	0.51	22.50	8.82	3.52	50.2 0	29.48	9.66
Pr	0.1	0.04	0.03	-	-	-	0.21	0.02	0.03	2.86	1.10	0.44	6.42	3.04	1.92
Nd	0.6	0.23	0.19	3.10	1.09	0.53	1.32	0.08	0.20	11.77	4.56	1.81	25.8 0	13.39	4.95
Sm	0.77	0.09	0.21	4.23	1.86	0.77	0.45	0.03	0.07	4.52	1.69	0.68	5.18	3.01	1.01
Eu	0.3	0.05	0.10	0.11	0.02	0.03	0.31	0.01	0.05	0.15	0.03	0.03	0.58	0.32	0.11
Gd	2.19	0.21	0.60	8.01	3.89	1.48	0.53	0.03	0.08	5.20	2.03	0.81	3.64	2.30	0.64
Tb	0.36	0.09	0.10	1.46	0.76	0.25	0.06	0.00	0.01	1.05	0.41	0.16	0.54	0.34	0.09
Dy	1.76	0.24	0.52	4.19	1.57	0.64	0.27	0.02	0.05	4.99	2.00	0.77	2.22	1.57	0.39
Ho	0.31	0.05	0.10	0.12	0.04	0.02	0.04	0.00	0.01	0.63	0.25	0.10	0.34	0.23	0.06
Er	0.76	0.09	0.20	0.17	0.02	0.03	0.08	0.02	0.03	1.31	0.53	0.20	0.86	0.55	0.15
Tm	0.09	0.02	0.03	0.01	-	-	0.01	0.00	0.00	0.14	0.06	0.02	0.12	0.08	0.02
Yb	0.45	0.11	0.15	0.18	0.03	0.04	3.00	0.09	0.46	0.85	0.35	0.13	0.71	0.47	0.12
Lu	0.06	0.01	0.02	0.02	0.00	0.01	0.01	0.00	0.00	0.10	0.05	0.02	0.11	0.07	0.02

Preprints (www.preprints.org) | NOT PEER-REVIEWED | Posted: 3 January 2024 doi:10.20944/preprints202401.0163.v1

∑REE	7.79	1.40	1.96	26.36	11.98	4.56	5.16	0.76	1.00	65.93	25.82	10.14	117.0	67.96	22.28
T Zrn (°C)	690	657	19.10	687	636	16.98	657	621	21.56	818	739	28.28	778	745	20.51
T Mnz	527	417	61.59	680	597	31.87	543	354	174.3	777	676	36.70	806	760	31.06
T Ap	1010	556	310.1	708	513	70.27	1049	759	145.8	894	672	89.42	811	637	129.1

Max: highest value; Av: average; Std: standard deviation; -: not determined or below detection limit; T_{Zrn}: saturation temperature of zircon according to the formulation of [57]; T_{Mnz}: saturation temperature of monazite according to the formulation of [58]; T_{Ap}: saturation temperature of apatite according to the formulation of [59].

3.2. The Golpejas Sn-Ta-Nb±Li Albite Granite

The Golpejas granite consists of several sheets of mineralized albitic granite with a semicircular shape [34] (Figure 1C). These sheets range from 7 to 35 m thick and dip outward from 30° to 72°. The grain size of the granite in these sheets varies from fine at the margins to medium grain in the central part. The presence of a subhorizontal foliation is prominent, especially in the deepest areas. The mineralization consists mainly of magmatic disseminated cassiterite and columbite group minerals in the leucogranite. In the north, where the highest tin and Nb-Ta grades are found, the granite is strongly kaolinized, resulting in high grades in most cases by mass loss [1]. Ore content can reach about 230 ppm for Nb and 215 ppm for Ta and up to 0.2% Sn (Table 2). The granite consists of quartz, albite, potassium feldspar and white mica as major minerals and zircon, cassiterite, Nb-Ta oxides, apatite and aluminum phosphates as accessory minerals. In the contact zone of this body with pelites, a greisen was developed with a thickness ranging from a few millimeters to 20 cm. Intragranitic quartz veins also occur containing Li minerals (amblygonite-montebrasite series), Cu, Sn, Zn, Ag and Bi sulfides, iron oxides and carbonates [34]. These quartz veins are often subhorizontal and subparallel to the granite foliation and occur mainly in the apical zone.

4. Methods

4.1. Mineral Chemistry

In this work, we have determined only the chemical-mineralogical composition of the Nb-Ta oxides and silicates of the Golpejas granite (Table S1); the rest of the data used in this work come from external sources (see Table 1).

Quantitative chemical analyses of Ta and Nb oxide minerals were carried out on carbon-coated thin sections using a JEOL Superprobe JXA-8900 M with WDS at the Electron Microscopy Service of the Complutense University of Madrid. The analytical conditions consisted of an acceleration voltage of 15 kV, a beam current of 20 nA, a beam diameter of 1-5 mm and counting times of 10 seconds. Standards used in analytical procedure include metals (W, Sn) zircon (Si, Zr), MnO_2 (Mn), LiNb (Nb), KaerTR (Na, Ca), hafnon (Hf), almandine (Fe), apatite (P, Cl, F), LiTa (Ta), UO_2 (U, Th) and IlmeTR (Ti).

A CAMEBAX SX-100 with WDS was also used to get quantitative chemical analyses of silicates at the Scientific-Technical Service of the University of Oviedo. The analytical conditions consisted of an acceleration voltage of 15 kV, a beam current of 15 nA, a beam diameter of 2 μm and counting times of 5 seconds. Standards used in analytical procedure include metals (Ni, Sn, W), orthoclase (K), andradite (Ca), MnTi (Ti, Mn), magnetite (Fe), albite (Na), jadeite (Si), Al_2O_3 (Al), MgO (Mg), apatite (P, F), chromite (Cr), vanadinite (Cl), covellite (Cu), Aspy_mac (As), celestine (Sr), Nb_mac (Nb), celsian (Ba) and Ta_mac (Ta).

Preprints (www.preprints.org) | NOT PEER-REVIEWED | Posted: 3 January 2024 doi:10.20944/preprints202401.0163.v1

4.2. Geothermobarometry

Thermometric estimates were constrained by the saturation of zircon [57], monazite [58], and apatite [59]. Pressure conditions were estimated using the phengite barometer [60] and, when available, reported microthermometric studies.

4.3. Water Content

Magma water content was estimated from the empirical model based on the H_2O (vapor) = H_2O (melt) equilibrium of [61] for an XH_2O in vapor of 1, pressure conditions estimated from the microthermometry, and thermometric estimates from zircon saturation. Samples showing kaolinization and phengitization were excluded.

4.4. Numerical Modeling

The liquid line of descent was performed using thermodynamic modeling with the Rhyolite-MELTS code [62], mass balance modeling with the OPTIMASBA code [63], and Rayleigh modeling with the FC-AFC-FCA code of [64].

5. Results

5.1. Mineral Chemistry

5.1.1. White Mica

The composition of the white micas of the Iberian rare-metal granites has been plotted in the diagram of [65], where most of the granites show Li-poor micas. Indeed, muscovite is the most abundant, with some occurrence in the phengite field (Logrosán, Penouta and Beariz granites) and in the Li-phengite field (Beariz and Golpejas granites). The Argemela granite is quite different, showing a very wide range of variation, with muscovite, Li-muscovite, Li-phengite, zinnwaldite and lepidolite (Figure 2A).

Preprints (www.preprints.org) | NOT PEER-REVIEWED | Posted: 3 January 2024 doi:10.20944/preprints202401.0163.v1

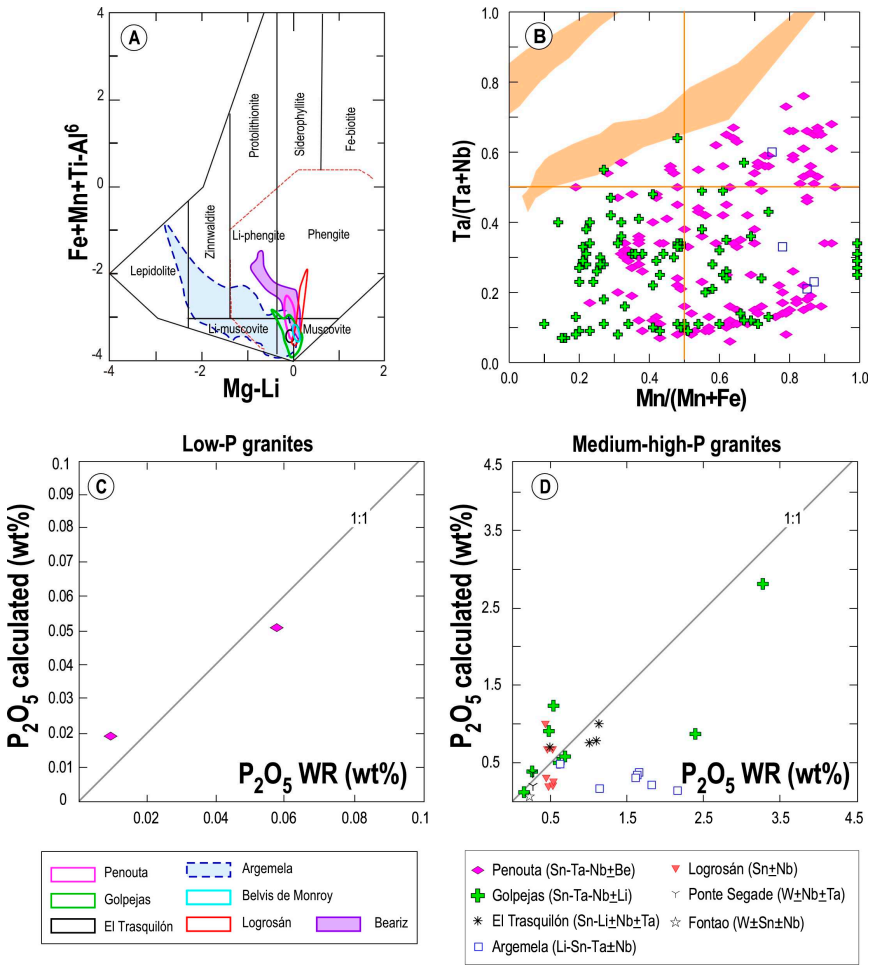

Figure 2. Mineral chemistry constraints. A) Classification of white micas for different Iberian rare-metal granites according to the diagram of [65]. B) Classification of Nb-Ta oxides in the CGM quadrilateral. Areas in orange represent compositional fields of cogenetic CGM and tapiolite according to [66]. C and D) P_2O_5 whole rock content vs. P_2O_5 calculated from P_2O_5 in alkali feldspar, applied to low-P rare metal granites (C) and medium- and high-P rare metal granites (D).

5.1.2. Alkali Feldspars

The potassium feldspar of Iberian rare metal granites is generally K-rich (99.4-77.8 Or%, average 96 Or%), Na-poor (21-0.5 Ab%, average 3.99 Ab%) and Ca-poor (1.49-0 An%, average 0.08 An%) (see Table S1). P_2O_5 contents in K-feldspar range from 1.5% to values below the detection limit of EMPA, with the Golpejas and Logrosán granites having the highest contents, i.e., both Nb-Ta rich and poor granites can have high P contents.

The plagioclase of the Iberian rare earth granites is always albite (3.47-0.03%An). The P_2O_5 contents range from 0.9% to values below the detection limit of the EMPA, with high values in both Nb-Ta rich and poor granites. It is noteworthy that P_2O_5 contents in plagioclase are lower than in K-feldspar.

The alkali feldspar composition was used to estimate the P calculated in the melt, to compare it with the actual P content of the whole rock, and to check whether P remained immobile or was mobilized by the fluids or a filter-pressing process (Figs. 1C and 1D) (see [67,68]). With respect to P-low granites, as in the case of Penouta, there are no significant differences between calculated and real P, so it can be concluded that P mobilization processes by fluids or filter pressing are negligible. With respect to the medium to high P granites, the Nb-Ta-poor granites such as Fontao, Ponte Segade and Logrosán generally do not show large differences between the calculated and actual P content of the rock, suggesting that there has been no significant mobilization of P by fluids, except for some

Preprints (www.preprints.org) | NOT PEER-REVIEWED | Posted: 3 January 2024 doi:10.20944/preprints202401.0163.v1

data from Logrosán that could be explained by some type of mobilization. With respect to the Nb-Ta-rich granites, Argemela shows a clear situation of disequilibrium, either by fluid mobilization of P from the feldspars, or by entry of P into the system also by fluids. In the case of the Nb-Ta-rich granite of Golpejas, there are samples that behave like a system in equilibrium, but others that clearly do not, with a loss of P from the alkali feldspars by fluids. In this granite there is also a calculated P enrichment with respect to the real one, which could indicate that there has been a loss of P from the system by filter-pressing [67].

5.1.3. Columbite Group Minerals

The disseminated ores of Nb-Ta oxides of the Iberian rare metal granites (Penouta, Argemela and Golpejas, i.e., Nb-Ta-rich granites) mostly correspond to the columbite supergroup, namely the Columbite Group Minerals (CGM) (Figure 2B). In the Penouta deposit, microlite, wodginite and ferrotapiolite have also been reported [3,4]. In the CGM, columbite (i.e., oxides with Ta*<0.5, with Ta* = Ta/(Ta+Nb)) is more abundant than tantalite (i.e., oxides with Ta*>0.5), the former being particularly abundant in Golpejas, where it can reach 95%. The Penouta deposit, on the other hand, is the one where tantalite is more abundant, reaching 33%. Manganese rich CGM (Mn* > 0.5, where Mn* is equal to Mn/(Mn+Fe)) are very abundant in Argemela (100%) and Penouta (73%), whereas iron rich CGM (Mn*<0.5) are predominant in Golpejas, where 66% of the available analyses correspond to ferrous CGM. Given the experimental work on tantalite [69–71], which shows that tantalite would form in a more evolved melt than columbite, it could be inferred that the Penouta melt would be the most evolved of the Iberian rare metal granites. Nevertheless, other options are possible, such as fluids that mobilize more Nb than Ta (as could also occur in the apical part of Penouta, [4]), or by the greater availability of P in Golpejas, which would favor more insoluble Ta than Nb [72], enriching the residual melt in Nb and not in Ta, that is, the opposite of what would occur in Penouta.

5.2. Whole Rock Geochemistry

5.2.1. Major Element Compositions

Iberian rare-metal granites have silica contents ranging from 63 to 77 weight percent (Figure 3), with the lowest values typical of the border facies, which can be either albite-rich and/or mica-rich (see [5,20]). Al_2O_3 is also quite variable, ranging from high concentrations (24 wt.%) in the Golpejas granite to 13 wt.% in quartz-rich samples from the Penouta albite granite (Figure 4). Most samples are peraluminous (average A/CNK = 1.33), although there are exceptions with values below 1 in P-Ca-rich samples from Golpejas (Figure 3A and F), although the latter reach values >1 when P is removed, as in the diagram of [73] (Figure 3 B). The low Ti, Fe, Mg and Mn contents of these granites, often below the detection limit, are typical of highly evolved magmas, with very limited femic minerals, restricted to ore minerals and Fe oxy-hydroxides. P_2O_5 contents vary between low to high phosphorus granites according to [71]. It is noteworthy that the phosphorus-rich samples from Golpejas granite have higher CaO contents than other analogous P-rich rare-metal granites as Argemela (Figure 4 and Table 2), probably because in Golpejas the predominant phosphate is apatite, while in Argemela the minerals of the amblygonite-montebrasite series dominate. The K_2O contents are typical of magmas with calc-alkaline to high-K calc-alkaline affinities (Figure 4). Granites are calcic to alkalic according to the MALI index and both ferroan and magnesian ([74]; Figure 3C, and 3D). Iberian rare metal granites are mostly sodic in terms of Al-Na-K ternary plot (Figure 3E) and all may be classified as felsic peraluminous (Figure 3F). In addition, all samples fall into the syn-collisional granites in the Rb-(Y+Nb) diagram of [75] (Figure 3G), ruling out that they are A-type granites according to [25]. Harker variation plots generally show poor correlation and only an acceptable negative correlation is observed with Al_2O_3 (Figure 4). Regarding the evolution by plutons, only a good correlation in Ca and P is observed for the Penouta granite in Harker variation diagrams.

Preprints (www.preprints.org) | NOT PEER-REVIEWED | Posted: 3 January 2024 doi:10.20944/preprints202401.0163.v1

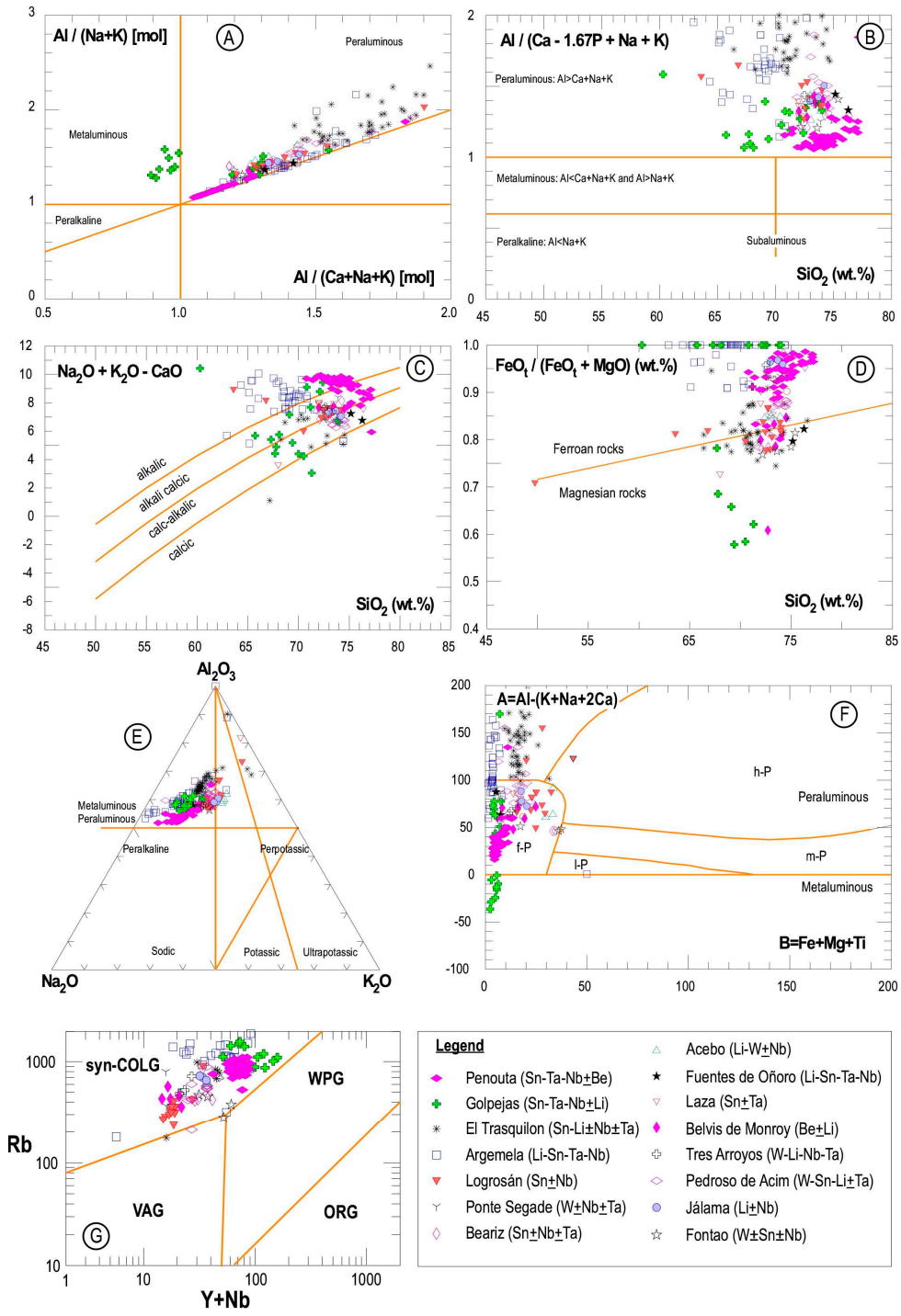

Figure 3. Classification diagrams. A) Diagram of [76] applied to Iberian rare metal granites. B) SiO_2- Aluminium saturation index plot of [73]. C) SiO_2- MALI (Na_2O+K_2O-CaO) plot of [74]. D) SiO_2- FeO^*_t plot of [74]. E) Molar Na_2O-Al_2O_3-K_2O plot to distinguish meta-/peraluminous from peralkaline rocks as well as potassic, sodic and ultrapotassic rocks. F) A-B multicationic plot of [77], modified by [78]. G) Y+Nb-Rb plot after [75]. L-P: low peraluminous; m-P: moderately peraluminous; h-P: highly peraluminous; f-P: felsic peraluminous; syn-COLG: Syn-colisional granites; WPG: within plate granites; VAG: volcanic arc granites; ORG: ocean ridge granites.

Preprints (www.preprints.org) | NOT PEER-REVIEWED | Posted: 3 January 2024 doi:10.20944/preprints202401.0163.v1

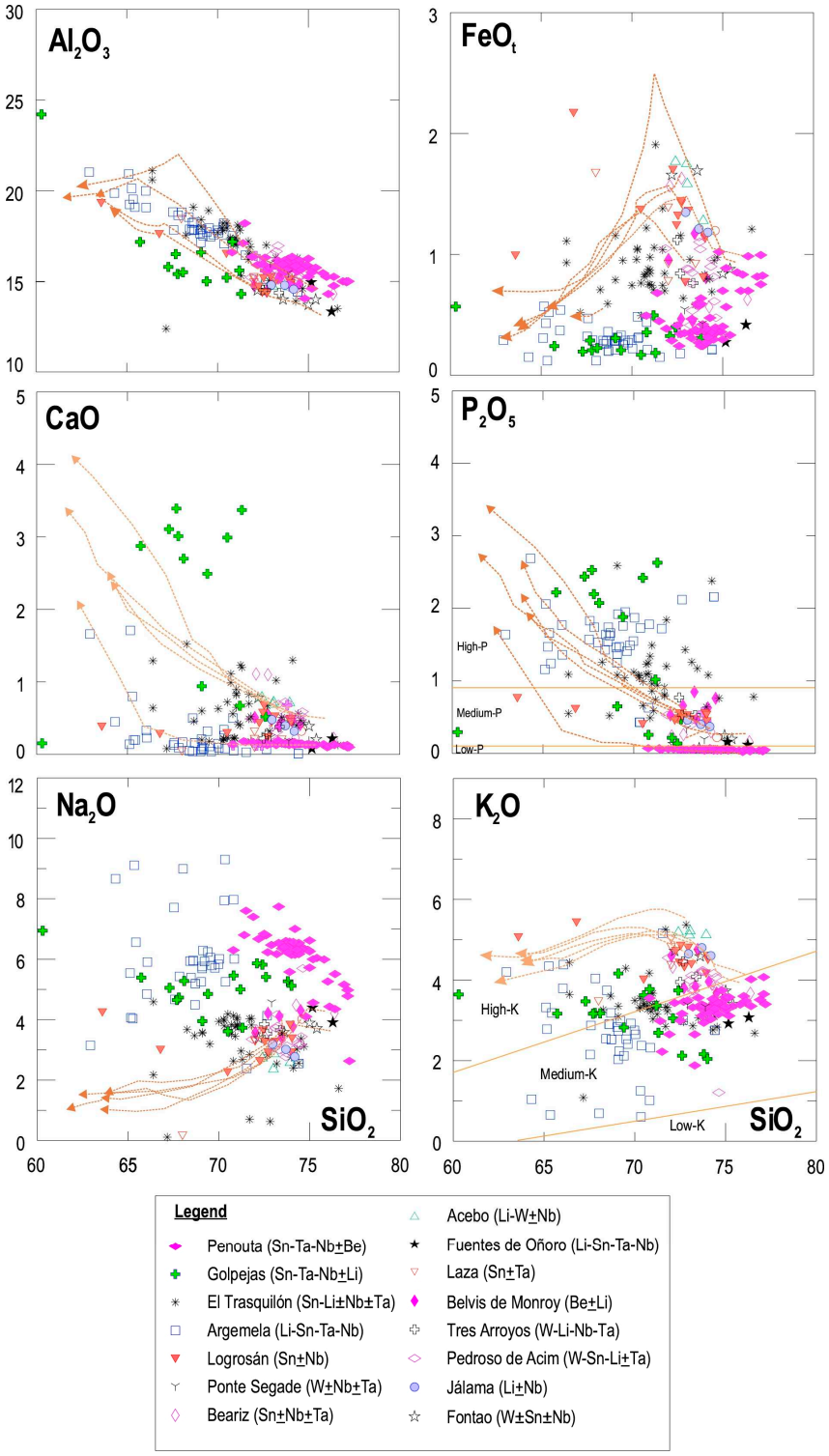

Figure 4. A-D) Harker variation diagrams. All figures in % by weight. Evolutionary paths carried out by Rhyolite-MELTS [62] were included, using tourmaline, two mica and cordierite-bearing granites as initial melts, a pressure of 300 MPa and a Ni-NiO buffer. Subdivisions of [79] in the K_2O plot are also included.

5.2.2. Trace Element and REE Concentrations

In the Iberian rare metal granites, the HFSE, namely Zr, Hf, Ta, Sn, Nb, U, W, and REE, are strongly controlled by accessory minerals. In this regard, the columbite group minerals of Nb-Ta-rich granites host mainly Nb and Ta, with high Ta contents in the Villardeciervos (up to 273 ppm), Penouta (up to 226 ppm) and Golpejas (up to 215 ppm) granites (Tables 1 and 2). The Nb/Ta ratio is

Preprints (www.preprints.org) | NOT PEER-REVIEWED | Posted: 3 January 2024 doi:10.20944/preprints202401.0163.v1

rather low (average 1.4), with the highest values in Nb-Ta-poor granites (close to 7 in the Logrosán granite), where CGM are absent, and values < 2 in Nb-Ta-rich granites, where CGM are present (Figs. 5 and 8). The opposite is true for the Ta/Nb ratio (Figure 8).

Sn is mainly hosted in cassiterite and to a lesser extent in stannite and varlamoffite. Sn is highly enriched in greisen or quartz veins of Sn granites (up to 7,201 ppm) and can show values up to 3,800 ppm as disseminated mineralization in Nb-Ta-rich granites (e.g., Penouta), although the latter can also show low values (20 ppm in Golpejas) (Figure 5).

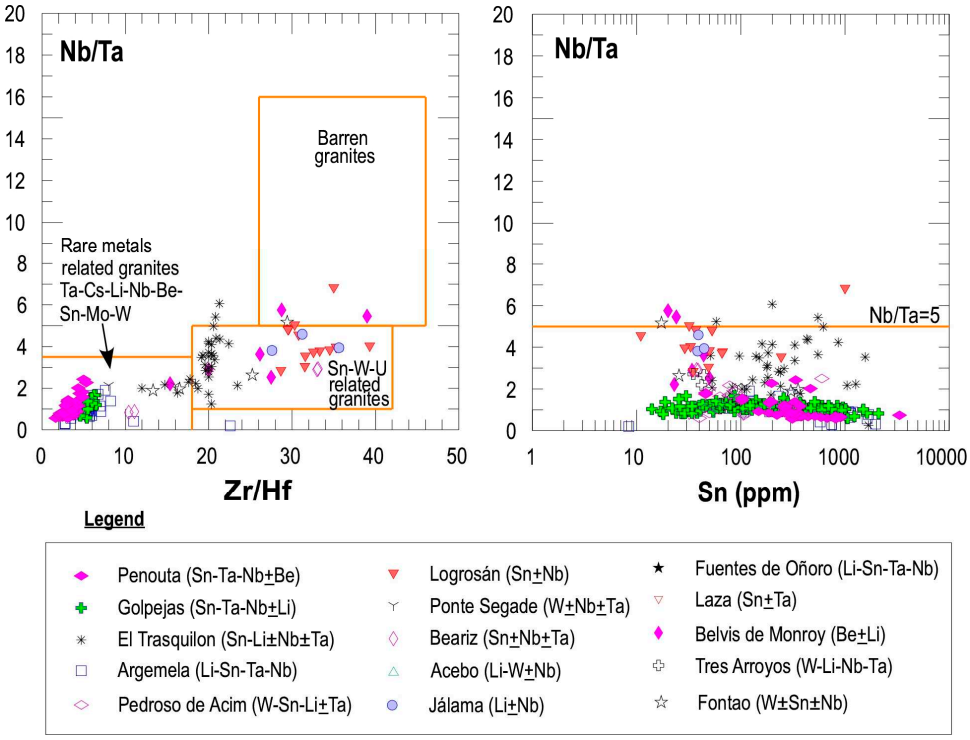

Figure 5. Evolution of Nb/Ta ratio as a function of Zr/Hf and Sn (from [80]).

The Zr content is mostly hosted in zircon. This element is high in the Nb-Ta-poor granites (up to 118 ppm in the Logrosán granite see Table 2) and distinctly low in the Nb-Ta-rich granites, with values up to 39 ppm in the Golpejas granite and as low as 10 ppm in the Argemela granite (Figure 5 and see Table 2). On the contrary, the Hf values (also hosted in zircon) are high in the Nb-Ta-rich granites (up to 8.5 ppm, in the Penouta granite) and typically low in Nb-Ta-poor granites (maximum value of 3.1 ppm in the Logrosán granite) (see Table 2). Regarding the Zr/Hf ratio, there is a clear contrast between Nb-Ta-poor granites, with values greater than 10, and Nb-Ta-rich granites, with values less than 8 (Figure 5), mainly because the latter are richer in Hf. U abundance (50–0.7 ppm, average 11 ppm) is higher than the upper lithosphere Clarke value (av. 2.7 ppm), indicating a ''fertile'' source of U. The highest U contents were found in the El Trasquilón (up to 50 ppm) and the lowest in the Logrosán granite (Table 2).

It should be stressed the high abundance in certain LILE elements, especially Rb (up to 2,448 ppm, average 920 ppm, and with the highest values in the Nb-Ta-rich granites (Argemela granite, Table 2), Cs (up to 350 ppm in the Argemela granite, average 57 ppm; Table 2), and Sr (up to 677 ppm in the border facies of Argemela, average 39 ppm, Table 2). The high Ga contents are noteworthy (Table 2), especially in Nb-Ta-rich granites, (up to 329 ppm in the Golpejas granite). Li contents are significantly high in the granites of Fuentes de Oñoro (8300 ppm), Argemela (5532 ppm) and El Trasquilón (4555 ppm). Sometimes, as in the Golpejas granite, the granite has low Li values (86 ppm on average, maximum of 1084 ppm, Table 2), but they have intragranitic veins rich in montebrasite. It should be noted that Be is present in significant amounts, as in the Argemela granite (up to 385 ppm), Penouta (up to 125 ppm), the Golpejas granite (up to 103 ppm), and the Beariz granite (up to 91 ppm), which according to [81] would be Be-bearing granites.

Preprints (www.preprints.org) | NOT PEER-REVIEWED | Posted: 3 January 2024 doi:10.20944/preprints202401.0163.v1

Fluorine data are scarce, but some Nb-Ta-rich granites, such as the Golpejas and Argemela granites, can reach up to 1.6% and 1.3%, respectively, and always with lower values in the Nb-Ta-poor granites (up to 0.58% in the El Trasquilón granite) (Table 2).

Upper crust normalized patterns of Nb-Ta-rich granites granites display positive peaks in Rb, U, Ta, Nb and Hf, and occasionally in some REE (Gd, Tg, Dy, Ho) and negative anomalies in Ba, Th, La, Ce, Pr, Nd and Ti (Figure 6). In contrast, Nb-Ta-poor granites (e.g., Logrosán, and Fontao) show positive peaks in Rb, U and Ta and sometimes in some REE, and negative anomalies in Ba, Th, Sr, Eu, Ti, La and Ce. It is worth noting that the REE content is usually lower than the upper crust content (Figure 6).

The REE patterns are variable (Figure 7) in the Nb-Ta-rich granites, with typical M-shaped tetrad patterns in the Penouta granite and very irregular patterns in the Golpejas and Argemela granites, in addition to low REE contents and a distinct tetrad effect in most of them (Figure 7). In contrast, Nb-Ta-poor granites exhibit more uniform geometries, a pronounced Eu anomaly, and a low tetrad effect (Figure 7). The ∑REE content is distinctly low in Nb-Ta-rich granites (up to 0.08 ppm in the Golpejas granite) with values increasing in Nb-Ta-poor granites (up to 117 ppm in the Logrosán granite) (Table 2). The REE fractionation $(La/Yb)_N$ is generally low, being higher in Nb-Ta-poor granites (up to 33 in the Logrosán granite) than in Nb-Ta-rich granites (up to 0.03 in the Argemela granite). Most samples show a weak negative Eu anomaly (Eu/Eu* average 0.46), with an occasional positive Europium anomaly (Eu/Eu*=1.94 in the border facies of the Argemela granite).

5.2.3. Isovalent Trace Element Ratios and Lanthanide Tetrad Effect ($TE_{1,3}$)

Typical isovalent trace elements such as Zr, Hf, Y and Ho and the lanthanide tetrad effect were used to decipher whether twin pairs such as Zr-Hf and Y-Ho show chondritic ratios (CHARAC behavior) typical of pure silicate melts, or non-chondritic behavior, as a result of fractionation in aqueous media or in high silica magmatic systems enriched in water, Li, B, F, P and Cl [82]. These twin pairs were also compared with the Nb/Ta ratio, which is typical of pure magmatic systems with values higher than 5 [80].

The Zr/Hf ratio varies widely from Nb-Ta-poor granites, where it can be chondritic, to Nb-Ta-rich granites, all of which have subchondritic values (Figure 8). In Nb-Ta-poor granites, although the Zr/Hf ratio varies widely, there is little tetrad effect and the Y/Ho ratio varies little, which is chondritic. However, in Nb-Ta-rich granites, the Y/Ho ratio and the tetrad effect have a very large range of variation, with a limited Zr/Hf ratio. On the other hand, the Nb/Ta ratio tends to behave analogously to the Zr/Hf ratio, with a very significant variation in Nb-Ta-poor granites and much less pronounced in Nb-Ta-rich granites.

Taking into account the values of chondrites, the limits of the CHARAC field, the field of no tetrad effect and the limit of the magmatic-hydrothermal environment in the Nb/Ta ratio (Figure 8), it is confirmed that Nb-Ta-poor granites are attributed to granitic melts following an evolution with little or no participation of fluxing elements. In contrast, the geochemical signature of isovalent trace element ratios and the lanthanide tetrad effect of Nb-Ta-rich granites are typical of a melt with an abundance of fluxing elements and with an important evolution in the magmatic-hydrothermal transition (see [80,82,83]).

Preprints (www.preprints.org) | NOT PEER-REVIEWED | Posted: 3 January 2024 doi:10.20944/preprints202401.0163.v1

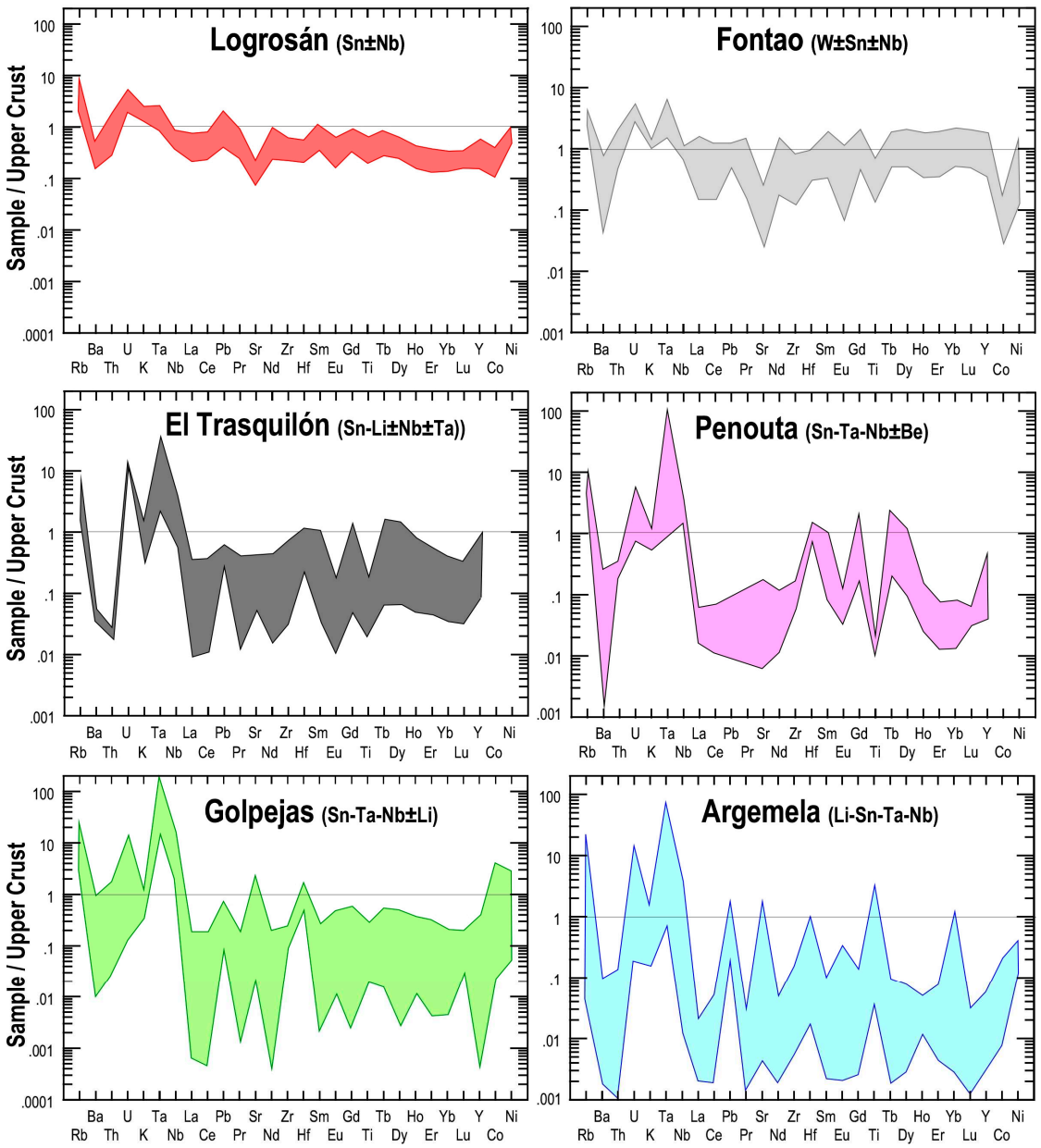

Figure 6. Spidergrams normalized to the upper crust from [83] and [84].

Preprints (www.preprints.org) | NOT PEER-REVIEWED | Posted: 3 January 2024 doi:10.20944/preprints202401.0163.v1

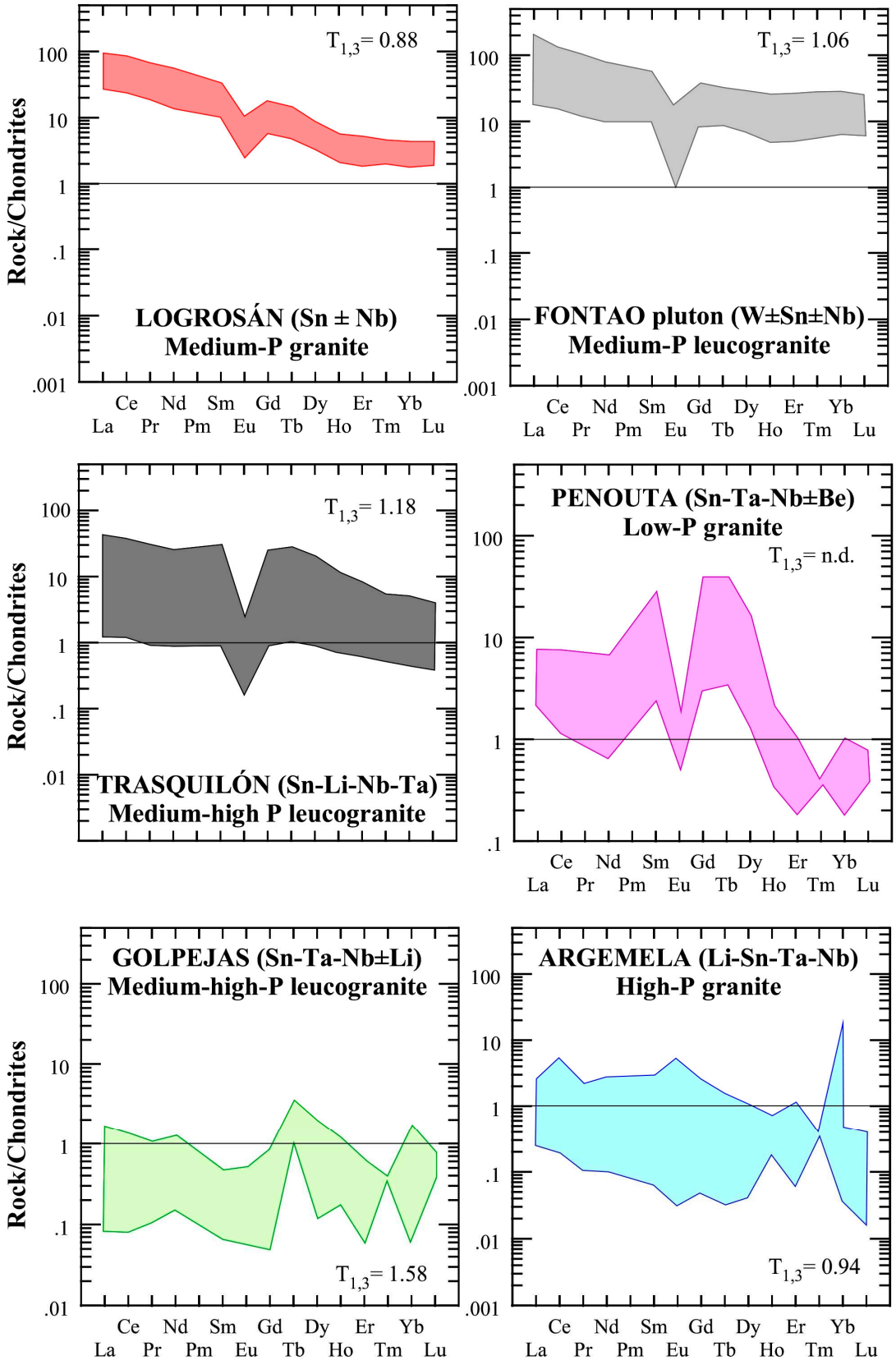

Figure 7. REE patterns normalized to the chondrite of [86]. Tetrad effect ($T_{1,3}$) is also included.

Preprints (www.preprints.org) | NOT PEER-REVIEWED | Posted: 3 January 2024 doi:10.20944/preprints202401.0163.v1

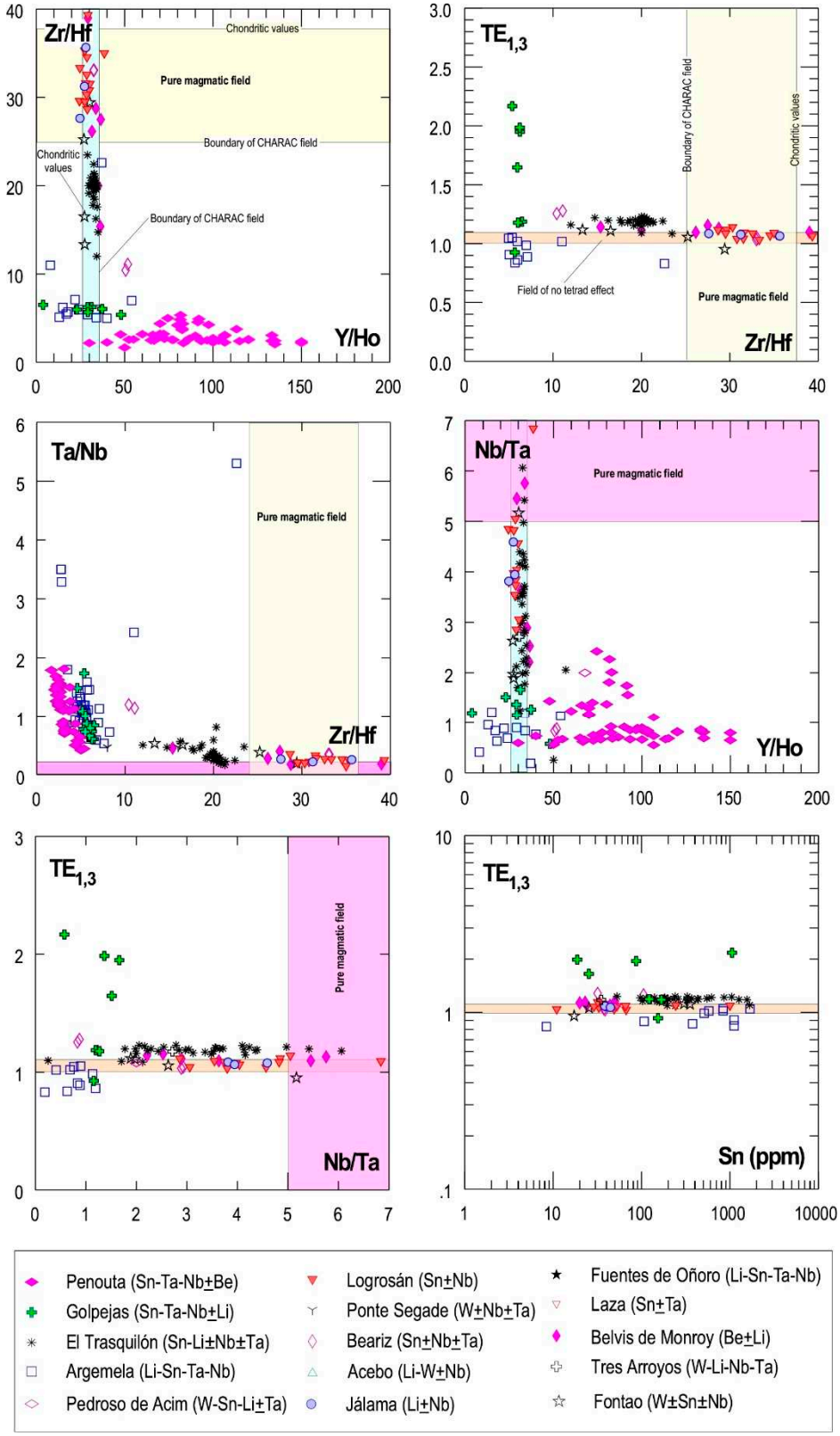

Figure 8. Binary plots showing ratios of isovalent trace element ratios and lanthanide tetrad effect ($TE_{1,3}$). The colored areas indicate domains of granitic melt evolution with little or no fluxing elements. The fields were constructed following [83] and [80].

5.2.4. Isotope Geochemistry

Isotopic data from Iberian RMGs are very scarce, only Sr-Nd data are available from granites from the central and southern part of the Central Iberian Zone, specifically from the plutons of: Sn-

Preprints (www.preprints.org) | NOT PEER-REVIEWED | Posted: 3 January 2024 doi:10.20944/preprints202401.0163.v1

Nb from Logrosán [35], Be±Li from Belvis de Monroy [52], and W-Li-Nb-Ta from Tres Arroyos [87]. The Logrosán granite shows a large variation in the initial $^{87}Sr/^{86}Sr$ ratios (0.7125-0.7286) and a restricted eNd (-4.0 to -4.3) (Figure 9). The Belvis de Monroy (border unit) also shows a restricted range of variation in the eNd (-5.34 to -6.18) and $^{87}Sr/^{86}Sr$ ratios more variable (0.7074-0.7215) (Figure 9). The Tres Arroyos granite show limited ranges of variation in the eNd (-3.42 to -5.17) and $^{87}Sr/^{86}Sr$ ratio (0.7125-0.7286) (Figure 9). All these values are quite similar to the wall rock of these granites, i.e. the Schist Greywacke Complex.

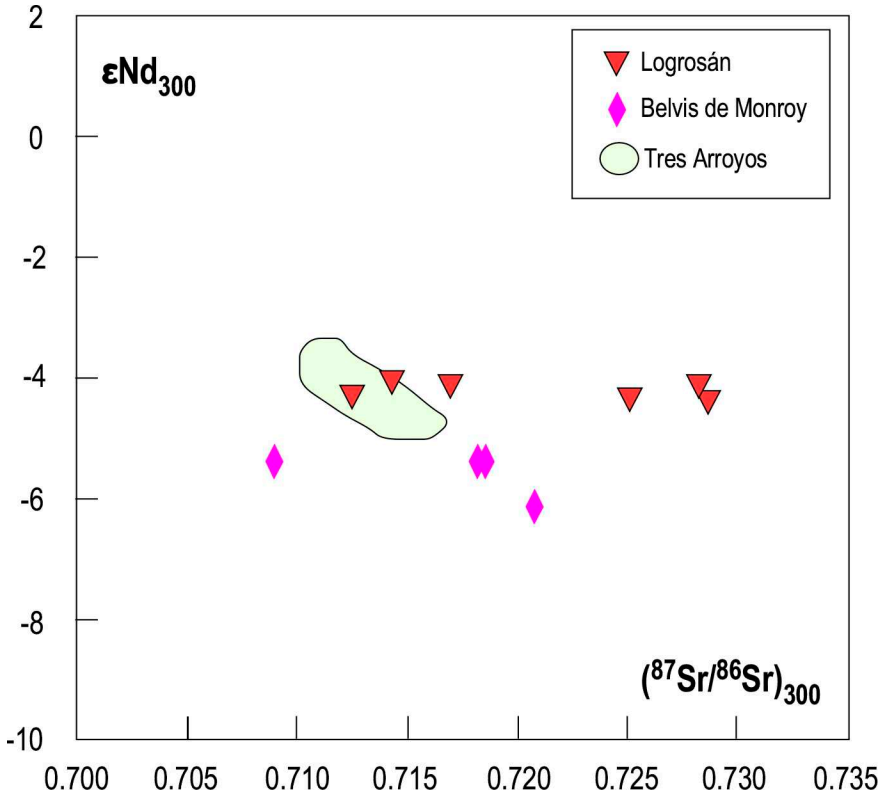

Figure 9. Sr-Nd diagram normalized to 300 Ma showing the isotope signature of the Logrosán [35], Belvis de Monroy (border unit; [52]), and Tres Arroyos (A unit of the Nisa-Alburquerque Pluton; [87]) plutons.

5.2.4. Geochronology

There are few dated Iberian rare metal granites. Among the Nb-Ta rich granites, the Argemela granite is the only one that has been dated, yielding an age of 326 Ma ± 3 Ma (U-Pb LA-ICP-MS in CGM, [88]), i.e. in the D2 age tectonic phase [29,89]. This age corresponds to the oldest known age of the magmatism that generated this type of RMG in Iberia. Among the Nb-Ta-poor granites, the oldest dated granite is the Belvis de Monroy granite (314 ± 3 Ma, U-Th-Pb ID-TIMS in monazite, [90]), corresponding to the D3 contractional deformation in the CIZ [29,89]. Finally, the younger recorded Nb-Ta-poor granite in Iberia is the Logrosán granite, which has an age of 307.9 ± 0.86 Ma (U-Pb ID-TIMS in zircon and monazite,[35]), coincident with the strike-slip shearing event in the CIZ [33].

5.3. Geothermobarometry

Geothermometric estimates of zircon, monazite and apatite saturation are shown in binary plots (Figure 10). There is only a good positive correlation between the saturation temperatures of zircon and monazite, and not in all cases. Nb-Ta-poor granites correlate in almost all cases, whereas Nb-Ta-rich granites correlate only in P-poor granites (Penouta) (Figure 10A). The apatite saturation model shows either too high (up to >1000 ºC) or too low temperatures (close to 250 ºC; Figure 10) and out experimental granite works for haplogranites (700-800 ºC, see [91,92]) and rare metal albite granite

Preprints (www.preprints.org) | NOT PEER-REVIEWED | Posted: 3 January 2024 doi:10.20944/preprints202401.0163.v1

melts (around 650 ºC, see [93]), suggesting that this thermometer generally does not work properly in most of our samples. It is worth noting that monazite saturation temperatures are too low in the phosphorus-rich Nb-Ta-rich granites, probably because there is no evidence of monazite in these granites [15,34], which is the case in the P-poor Nb-Ta-rich granite from Penouta [2], showing temperatures similar to those of zircon.

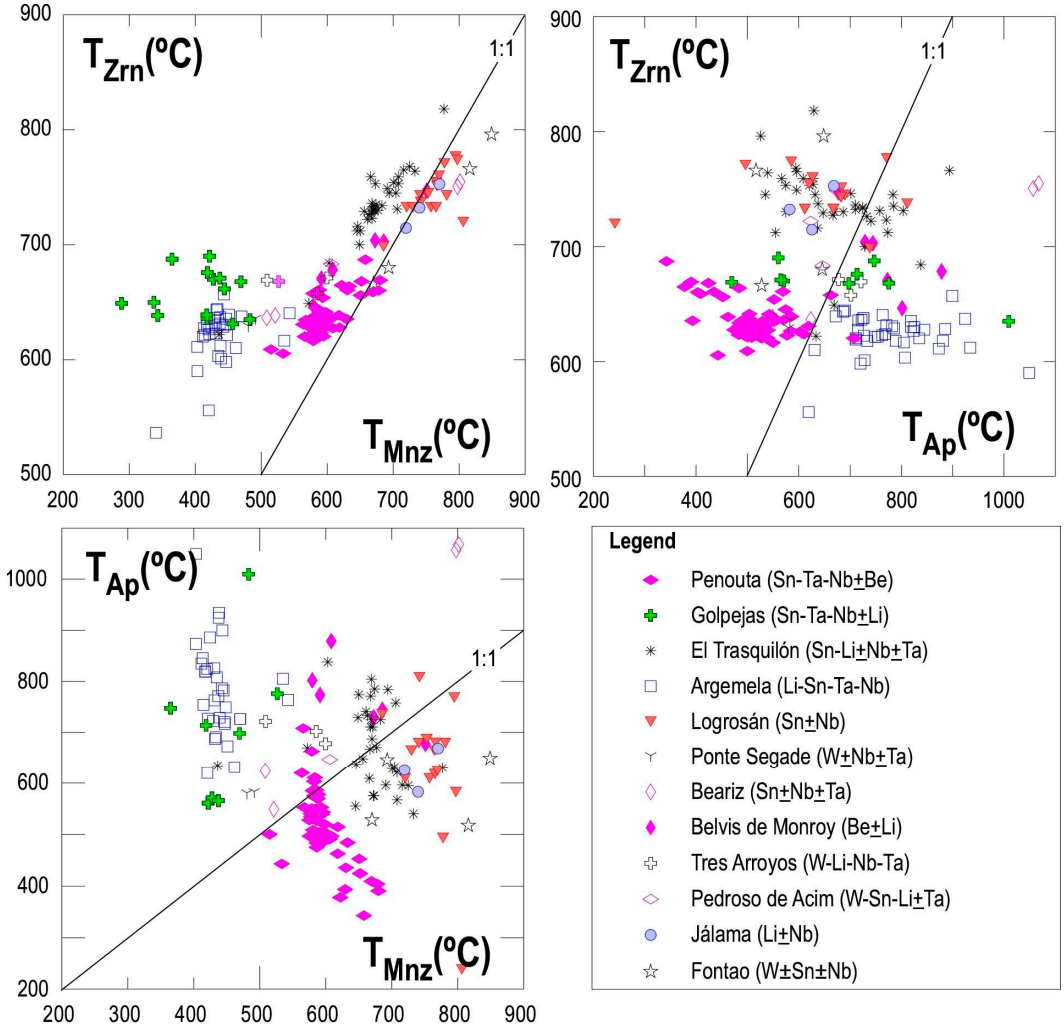

Figure 10. Zircon, apatite and monazite saturation temperatures calculated after the methods of [57–59] respectively.

Having made these considerations, and staying only with the saturation thermometer of zircon and monazite when there is evidence of their presence in the granite, it should be noted that the Nb-Ta-poor granites were emplaced between 800 and 700 ºC, while the Nb-Ta-rich granites were emplaced at a lower temperature (<700 ºC), reaching values as low as 600 ºC, which are quite similar to those reported for other Nb-Ta-rich granites, such as the Beauvoir granite from experimental approaches [93].

The geobarometry of these deposits is not straightforward due to the lack of suitable mineral associations. The exception could be the geobarometer using the chemistry of white mica (Si content of phengite, [60]). However, the results obtained for both phengite and muscovite white micas show variation ranges of more than 5 kbar for each deposit in primary white micas, which is the reason for not including the results. It was decided to take into account microthermometry studies reported for some of these deposits and to consider the trapping conditions of the first fluids of these deposits, especially for the formation of oxides (i.e. cassiterite), as a minimum emplacement value. These

Preprints (www.preprints.org) | NOT PEER-REVIEWED | Posted: 3 January 2024 doi:10.20944/preprints202401.0163.v1

values indicate that these granites were emplaced under shallow conditions (< 3 Kbar, Figure 11), especially in the Nb-Ta-rich granites (< 2 Kbar), being somewhat higher in the Nb-Ta-poor granites.

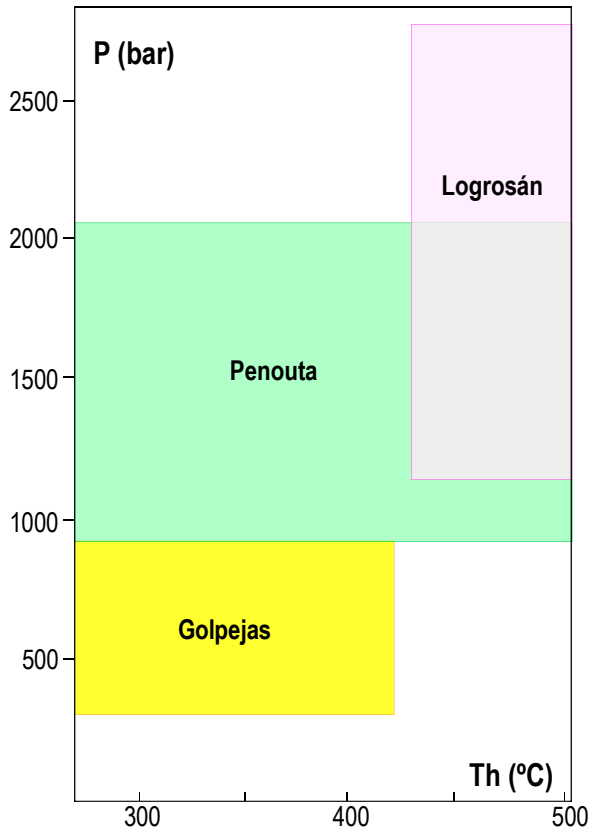

Figure 11. P-T reconstruction for trapping of the earliest fluids (cassiterite precipitation) in Nb-Ta-poor granites (Logrosán) and Nb-Ta-rich granites (Penouta and Golpejas). Penouta and Golpejas conditions from [94] and Logrosán estimates from [35].

5.4. Water Content

The results of the the H_2O (vapor) = H_2O (melt) equilibrium shows high H_2O contents in the rare metal granites, with values close to 6% for the shallow cooling conditions of these granites. It is noteworthy that Nb-Ta-rich granites have higher H_2O contents than Nb-Ta-poor granites (Figure 12 A and B).

Considering isobaric cooling (Figure 12A), the H_2O content increases slightly up to temperatures close to 600 ºC, i.e. close to the solidus, and then decreases. When the melt evolves by isothermal decompression, a loss of water in the melt is observed as the confining pressure decreases (Figure 12B). This behavior can lead to the separation of the fluid phase by first boiling [95,96]. It is observed that the loss of water in the melt by isothermal decompression is more pronounced than by isobaric cooling at temperatures close to the solidus (Figure 12B).

Preprints (www.preprints.org) | NOT PEER-REVIEWED | Posted: 3 January 2024 doi:10.20944/preprints202401.0163.v1

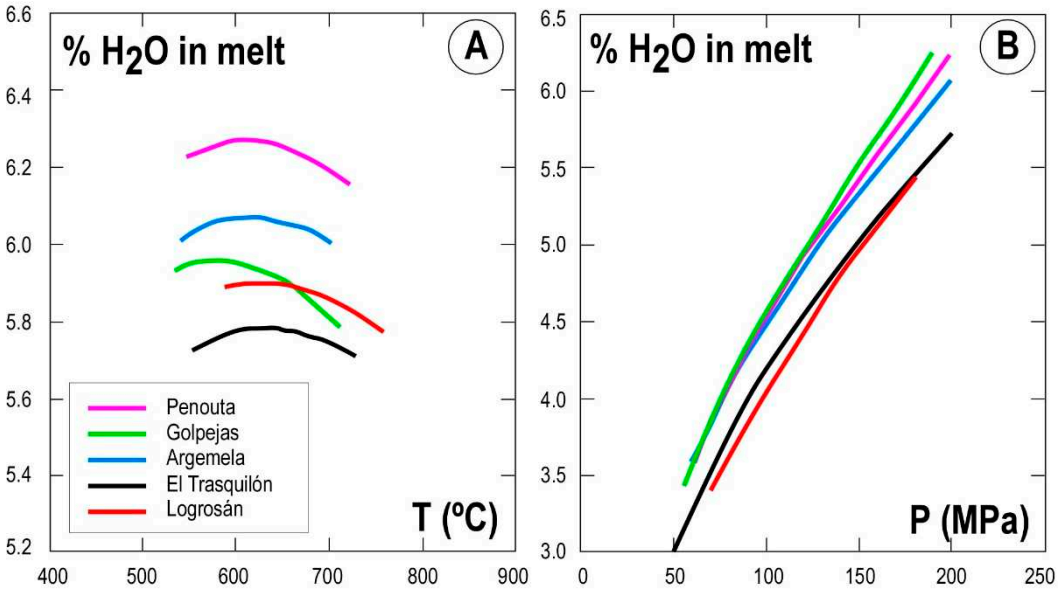

Figure 12. Melt water content versus temperature (A) and pressure (B) in selected rare metal granites. Pressure in A ranges from 100 MPa (Golpejas) to 200 MPa (the others). The temperatures used in B are those of zircon saturation (averages): 666 ºC (Penouta), 670 ºC (Golpejas), 637 ºC (Argemela), 716 ºC (El Trasquilón), and 782 ºC (Logrosán).

6. Discussion

6.1. The Parental Magmas of Iberian rare Metal Granites

The Iberian rare metal granites, like other rare metal granites worldwide, have a composition that has been explained by a process of extreme differentiation (e.g., [97,98]), melts from special protoliths plus fractional crystallization [6,99,100], and metasomatic processes [22,101,102,104]. The metasomatic processes that linked the chemistry of the RMGs to the destabilization processes of the biotite and feldspar from the root zones are now strongly disproved by the discovery of volcanic/subvolcanic equivalents (ongonites and macusanites) with identical compositions to the RMGs, the existence of experimental work that reproduces the chemistry of these granites from melts enriched in fluxing elements, and the existence of melt inclusion with this geochemistry [105]. While it is true that many of the rare metal granites show evidence of hydrothermal activity, this is more related to the evolution of the magma at the emplacement site (see below) that fluids of a depth origin. The possibility that these granites are derived from specialized protoliths is attractive because they require a smaller volume melting process and less fractionation to achieve the same level of enrichment compared to unenriched protoliths [106]. However, to achieve the high enrichments of rare metal granites, at least one extensive fractional crystallization process is required.

Most of the Iberian rare metal granites occur in isolated bodies with no apparent spatial relationship with other less evolved granites (Penouta, Golpejas, Argemela, El Trasquilón, Logrosán, Ponte Segade, Laza-Arcucelos, Pedroso de Acim, Belvis de Monroy, Acebo), which could indicate that there is no direct relationship with a less evolved parental magma. However, there are cases, such as the granites of Fuentes de Oñoro or Villardeciervos, where they are spatially associated with less evolved granites. Likewise, gravimetric surveys carried out in the Logrosán granite [47] and the existence of deep boreholes in the Golpejas [34] seem to confirm that there are less evolved granites at depth that could represent the parental magmas of these granites, reinforcing the hypothesis that GMRs are formed by a process of extreme differentiation.

A process of extreme differentiation from surrounding granites has also been invoked to explain the genesis of Iberian aplites and LCT pegmatites [107]. Indeed, these authors find geochemical affinities, especially in trace elements, between LCT pegmatites and two granite suites: two-mica granites and P-rich and highly peraluminous granites. From Figure 13 it seems plausible that there

Preprints (www.preprints.org) | NOT PEER-REVIEWED | Posted: 3 January 2024 doi:10.20944/preprints202401.0163.v1

could be geochemical affinities between rare metal granites and different Iberian granitic types, and this affinity can be extended not only to two-mica granites and P-rich and highly peraluminous granites, but also to moderately peraluminous and P-poor granitoids (i.e., granodiorites), and it is not excluded that even I-type granites of low peraluminosity are involved (Figure 13). Indeed, considering the trace element chemistry of the low-P and Nb-Ta-rich Penouta granite, the latter may represent an evolved melt of granodiorites, which incidentally outcrop not too far from the Penouta granite (see [2]). Likewise, the subvolcanic margin facies of the Fontao granite has a Th- and Y-rich, and notoriously Ba-rich and P-poor chemistry, making it similar to the evolutionary trends of the I suite (Figure 13). However, the strongly W-Sn mineralized central facies of this granite loses the I-type signature, so a more detailed study of this granite, outside the scope of this work, needs to be done to explain this dichotomy and a possible provenance of type I granites. With the exception of the Penouta granite and the rim facies of the Fontao granite, the rest of the Iberian rare-metal granites have a chemistry similar to that of the evolved melts of the two-mica granites and the P-rich and highly peraluminous granites.

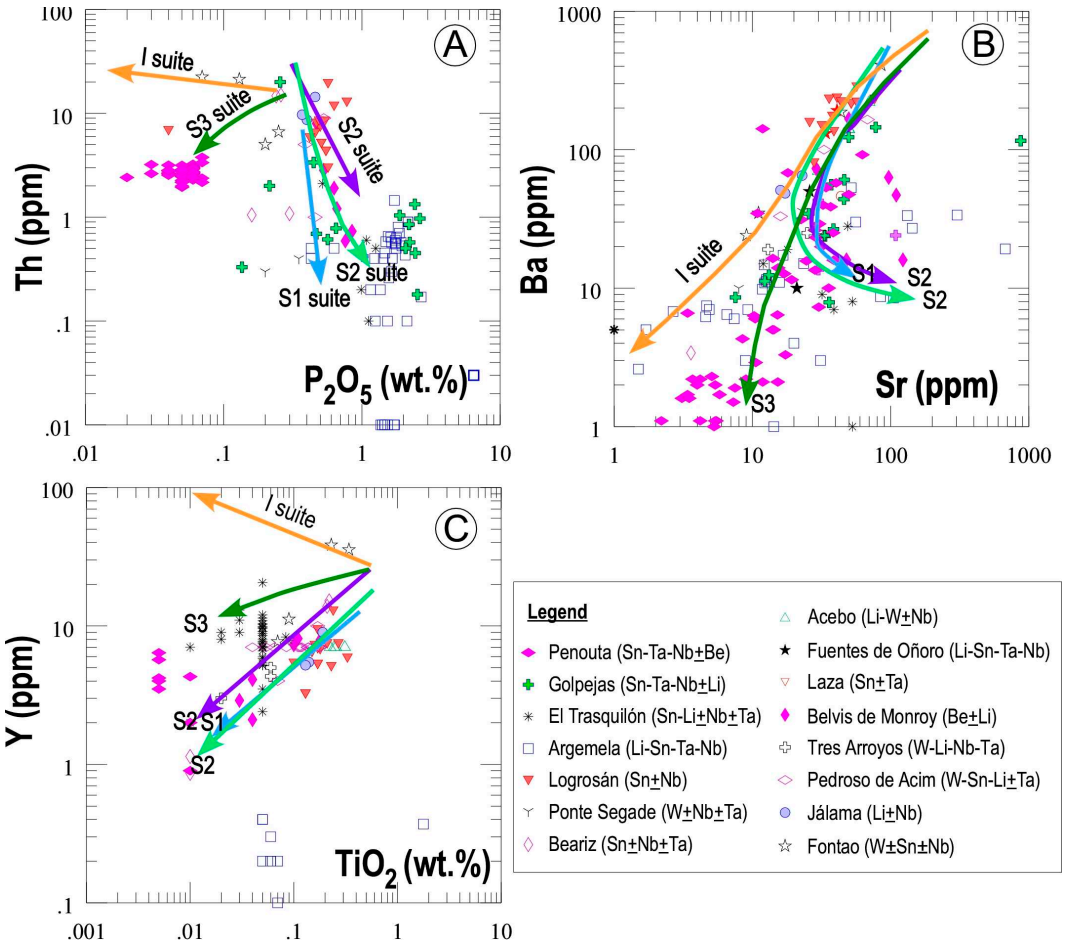

Figure 13. Typical chemical trends in Iberian granite suites derived from CIZ granites and aplite pegmatites according to [107]. The S1 suite corresponds to the two-mica leucogranite suite, the S2 suite to the P-rich highly peraluminous granite suite, the S3 suite to the P-poor moderately peraluminous granite suite, and the I suite to the low peraluminous I-type granite suite.

6.2. Chemical Evolution in Iberian RMGs

As seen above, the RMGs appear to be derived by a process of differentiation from some surrounding granites. Having a compositional starting point allows us to address an issue that is not entirely clear for RMGs: what is their geochemical evolution in a purely magmatic system, allowing us to evaluate possible deviations due to other processes.

Preprints (www.preprints.org) | NOT PEER-REVIEWED | Posted: 3 January 2024 doi:10.20944/preprints202401.0163.v1

A good tool to address this issue is thermodynamic modeling, e.g. Rhyolite-MELTS [62], by considering as parental magmas surrounding granites, such as two-mica granites, tourmaline-bearing leucogranites, P-rich and very aluminous granites (cordierite-bearing), and muscovite-rich granites. The Rhyolite-MELTS liquid lines of descent show that the evolution is to depletion in silica and Na, enrichment in Al, Ca and P, and shows an initial enrichment and then depletion in Fe and K (Figure 4). The samples that best fit this theoretical evolution are undoubtedly the rim-facies granites of Argemela (aplitic facies) probably because of their rapid crystallization, which avoided much interaction with the volatile phase and/or fluxing elements. and the Sn-W granite of Logrosán. The worst are the Nb-Ta-rich granites that are not rim facies. The modeling also clarifies that the high Al contents of some facies of these granites seem to be consistent with the evolution of the melt, and the same can be said for the high P contents (close to 3%) of the rim facies of the Argemela granite. In this sense, thermodynamic modeling shows that apatite is a phase that does not saturate or saturates very late in this kind of peraluminous granite melts, probably due to the scarcity of Ca in the system, explaining the high P contents in the most evolved melt.

Undoubtedly, the theoretical evolution of Na is the one that least fits the real samples (Figure 4). Thermodynamic modeling predicts that alkali feldspar is an early mineral in the crystallization sequence and that it consumes quite a lot of sodium from the melt, progressively depleting it. However, the real samples of Nb-Ta rich granites tend to be more enriched in Na in the poorer Si terms due to the abundance of albite. This discrepancy can be explained either by a superimposed albitization process, by the presence of fluxing elements, such as fluorine, in the system that modify the stability of quartz and enrich the residual melt in alkali feldspar [108], a combination of both processes, or undercooling disequilibrium crystallization [109]. Analyses of fluxing elements in Iberian RMGs are scarce, and those available (0.3% average F, maximum 1.6% in Golpejas; 0.1% average F, maximum of 0.5% in Logrosán, Table 2) do not reach the high fluoride contents necessary to significantly increase the stability field of quartz (2-4%, see [108]) and produce albite-rich melts via fluxes-rich melts. In some cases, such as the Golpejas and the El Trasquilón granites, some of this fluoride could have been removed from the magma by an exsolved fluid phase, since the deposits have montebrasite-rich veins [34,44], but there are cases, such as the Penouta granite, where this fluoride loss is not so easy to explain due to the absence of montebrasite and the extremely low amount of apatite [2]. What the available fluoride data seem to show is that the Nb-Ta-rich granites have significantly higher fluoride contents than the Nb-Ta-poor granites, where Na enrichment is not as pronounced. Moreover, the presence of alkali feldspars corroded by albite is the rule in RMGs, especially in Nb-Ta-rich ones [2,20], and it seems plausible that a superimposed albitization process enhances albite formation and also induces Na enrichment of RMG granites, namely Nb-Ta-rich ones. In addition, severe undercooling, as may have occurred at Golpejas, could lead to isothermal subsolidus fractional crystallization and a feldspar enrichment. In this scenario, a melt may remain metastable at temperatures below its thermodynamic solidus before crystallization begins, with the mineral with the highest chemical potential in this undercooled state crystallizing first, which in granite pegmatites is alkali feldspar due to its higher chemical potential in the undercooled state [109].

6.3. The Role of Fluids in the Crystallization of Iberian RMGs

The intensive variables as well as some geochemical and textural features of the Iberian RMGs suggest that these granites may have undergone fluid phase exsolution and in some cases may have enhanced rare metal grades to economic levels. The high water content of these granites, up to 6% in quite shallow conditions (Figure 12), is a critical factor in reaching saturation and causing separation of the fluid phase at an early stage relative to the crystallization progress [95]. In general, early saturation allows ore elements to be incorporated into the volatile phase from the outset, something that does not occur in undersaturated magmas, where ore elements can become part of the magmatic minerals, thus reducing the amount of ore elements that could pass into the volatile phase when saturation occurs [110].

Preprints (www.preprints.org) | NOT PEER-REVIEWED | Posted: 3 January 2024 doi:10.20944/preprints202401.0163.v1

There are two other mechanisms that allow the liquid phase to exsolve: isothermal decompression and isobaric cooling with crystallization of anhydrous phases. In an isothermal decompression scenario, the rise of a magma at lower pressures causes the amount of water dissolved in the melt to decrease dramatically (Figure 12B), favoring the saturation and exsolution of the fluid phase (first boiling). The low pressures estimated in the Iberian RMGs, especially those rich in Nb-Ta (<2 Kbar) suggest that isothermal decompression processes most likely occurred in the Iberian GMRs. The isobaric cooling mechanism (Figure 12A) is also very feasible, because most of the crystallizing minerals are anhydrous (modal contents of hydrated minerals are only of about 10% in Penouta and Argemela, [2,15]. This essentially anhydrous crystallization increases the volatile content in the melt until a point is reached at which the melt becomes saturated and the liquid is exsolved (second boiling), which is particularly easy in the shallower environments (e.g., Golpejas granite). Second boiling may be increased by strong undercooling especially in the border zones of the granite in contact with the colder wall rock. This phenomenon has been described in the lenticular granite of Penouta, both in the wall and roof zones, where volatile phase exsolution has been associated [2]. It is quite probable that this phenomenon also occurred in the tabular granite of Golpejas, which, due to its reduced thickness (maximum 30 m), must have been strongly undercooled in its apical and basal zones.

At the mesoscopic scale, we also find evidence of volatile phase saturation processes in the Iberian GMRs, such as the presence of greisen (Penouta, Golpejas), pegmatites interbedded with aplites in the apical part of the granite (e.g., Penouta, [2]). Also at the microscopic scale, the presence of snowball quartz with plagioclase microinclusions has been associated with the presence of an exsolved fluid phase [111], which could occur in the Golpejas, Penouta, and Argemela facies with this quartz type.

Whole-rock geochemistry also seems to support that the melt of the Nb-Ta-rich Iberian RMGs crystallized in a volatile-rich aqueous environment. Indeed, twinned elements such as Zr-Hf, Y-Ho and Nb-Ta show values far from chondrite (Figure 8) by fractionation in a fluid-rich environment, probably with abundance of fluxing elements and with an important evolution in the magmatic-hydrothermal transition [80,82,83].

Similarly, geothermometric constraints from the Golpejas granite also seem to support the involvement of a fluid phase at temperatures around 500ºC, as shown by Kfs-plagioclase and muscovite-plagioclase thermometers [112]. This fluid phase also seems to be responsible for the release of P (see Figure 2C and 2D), Ca and Na, among other elements, from the alkali feldspars, resulting in the strong enrichment of apatite and phosphates of Al, and possibly the formation of albitites in this granite. The strong P_2O_5 depletion calculated in the Argemela granite (Figure 2B) could also be interpreted in a similar way [20].

6.4. Ore Formation in Iberian RMGs

6.4.1. Sn-Nb-Ta-Rich Granites

The Iberian Nb-Ta-rich RMGs where the ore genesis is best known are the Penouta and Argemela granites. In the Argemela granite significant LA-ICP-MS characterization of micas and quartz has been carried out [5,20], which has allowed to investigate the genesis of the ore from a magmatic stage to a hydrothermal event. According to [5], the evolution of the ore (Li, Sn, Nb and Ta) is very well explained according to a magmatic model in which the saturation of accessory phases, first of montebrasite, then of cassiterite and finally of CGMs, plays a relevant role in explaining the decrease of Li, Sn, Nb and Ta in muscovite and in the melt itself. In contrast, the evolution of W cannot be explained by the saturation of wolframite in a magmatic system, and a magmatic fluid phase is involved to which W would migrate, since the fluid/melt partition coefficient of this element is significantly high (15).

In the Penouta granite, the crystallization of CGMs is purely magmatic, as is most of the cassiterite, which seems to be partly related to the involvement of an exsolved fluid that causes the highest Sn enrichments, both in the granite (central part in association with Be) and in the

Preprints (www.preprints.org) | NOT PEER-REVIEWED | Posted: 3 January 2024 doi:10.20944/preprints202401.0163.v1

metamorphic wallrock of the top, where a Sn-rich greisen is formed [2]. Based on mass balance and Rayleigh fractionation models, these authors develop a model that explains the variation of the Ta/Nb ratio in the whole rock from the bottom of the granite (rich in white mica) to the more Ta-enriched apical part, which is poor in white mica. In this model, white mica fractionates from the bottom to the top and plays a very important role as a fractionation phase, since this mineral fractionates more Nb than Ta [113], by fitting the theoretical model to the real samples without including other fractionation phases of Nb with respect to Ta, i.e., CGM. The above, together with the fact that no inflections in Ta and Sn are observed in the whole-rock variation diagrams, suggests that saturation of tantalite and cassiterite, both crystallizing in a trapped melt, has not occurred. This late crystallization would be supported by the high solubility of tantalite in experimental approaches in haplogranite melts and melts with fluxing elements [114–118] and the composition of CGM itself in the CGM quadrilateral (Figure 2B), with a majority composition in intermediate positions between columbite and tantalite, which has been interpreted in the context of local supersaturation processes [3].

The role of micas in the evolution of Nb and Ta in Iberian RMGs seems to be important. The evolution of Nb and Ta largely depends on the amount and type of mica removed, according to mass balance and Rayleigh fractionation modeling performed in Figure 14. Thus, the Pedroso de Acim granite has the highest slope in the Ta/Nb ratio, removing micas (biotite and white mica) in a sum of 28%. It is followed by the Penouta granite, and finally by the Golpejas granite, with the lowest slope. These last two granites fractionate only muscovite, while the Penouta granite does so to a greater extent (21% vs. 9% in the Golpejas granite), which explains its greater slope in the Ta/Nb ratio. It should be noted that there is significant scatter in the Golpejas granite, suggesting the involvement of processes other than white mica fractionation, e.g., exsolved volatile phase, which distort the overall evolution.

On the other hand, the existence of CGM with sponge-like textures in the apical part of granites, such as Penouta [4], has led some authors to consider the existence of a fluid phase capable of attacking a very acid-resistant mineral such as CGM. Acidic fluids appear to mobilize more Nb than Ta [119], which opens the door to the possibility that the interaction of these fluids could explain the sponge-like textures and the existence of Ta-rich CGM in the apical granite in addition to an upward migrating Nb-rich fluid.

Preprints (www.preprints.org) | NOT PEER-REVIEWED | Posted: 3 January 2024 doi:10.20944/preprints202401.0163.v1

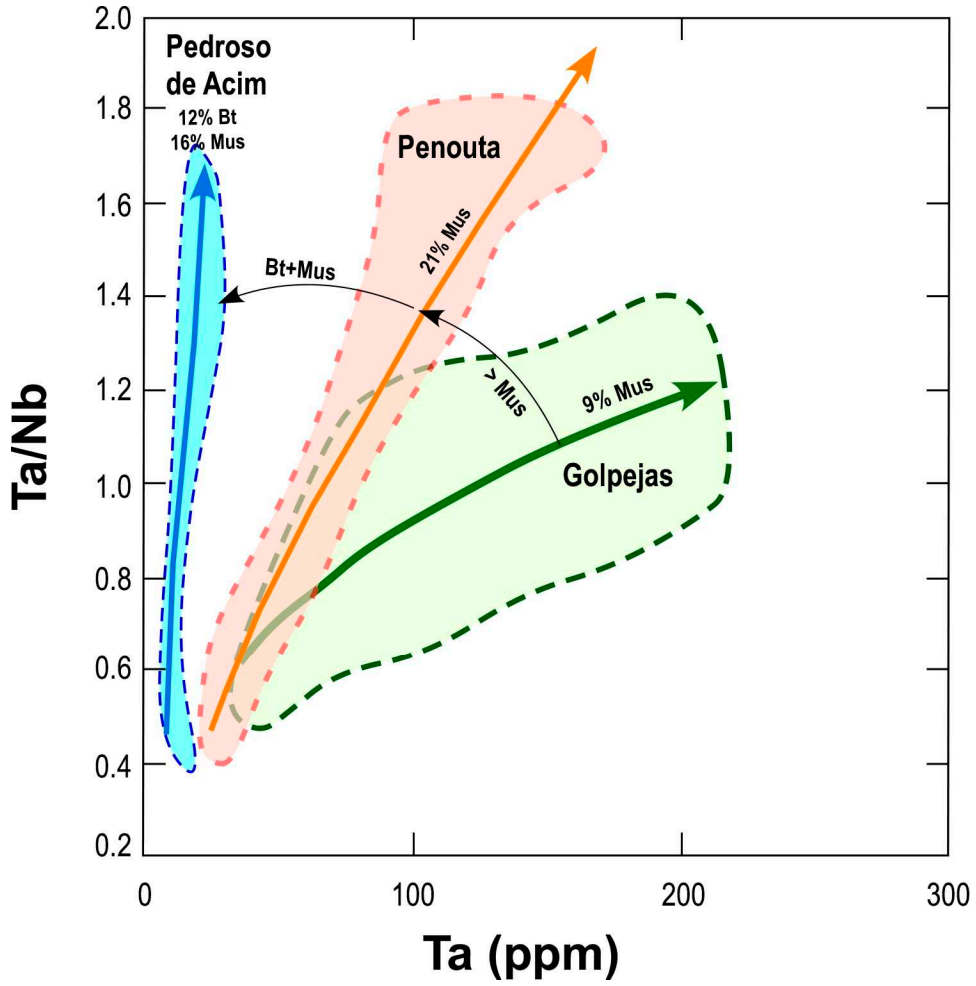

Figure 14. Ta vs. Ta/Nb ratio for three Iberian RMGs (Pedroso de Acim, Penouta, and Golpejas) showing Rayleigh fractionation modeling using the mode obtained by mass balance modeling (only mica cumulate mode is shown in the figure). The partition coefficients for Nb and Ta in muscovite are taken from [113], for biotite from [120]. Penouta data are from [2], Golpejas data are from [38,39], and Pedroso de Acim data are from [44,53].

6.4.2. Nb-Ta-Poor Granites

The best studied Nb-Ta-poor granite is from Logrosán [35,47]. The mineralization consists of stockworks and disseminations in altered rocks (endogreisen and wall rock), enriched in Sn and slightly enriched in Nb-Ta, in the so-called oxide-silicate stage. In this stage, Nb-Ta oxides precipitated first and then cassiterite according to the paragenetic sequence. This stage is related to the mixing of magmatic and metamorphic fluids, which increased the fO_2 and triggered the precipitation of cassiterite. It is worth mentioning that the granite melt must have contained a large amount of B, as abundant small q-tourmaline veins without preferred strain and tourmalinization occur in the granite and in the host rock, typical of B-rich melts and boron-dominated greisen deposits. This type of deposit has a high volatile content, which triggers the faulting of the cupola and enhances fluid exsolution and ore mobilization.

7. Conclusions

The main features of this work are summarized as follows:

(1) The Iberian rare metal granites can be divided into Nb-Ta-rich and Nb-Ta-poor granites in view of their contrasting intensive variables and geochemistry.

Preprints (www.preprints.org) | NOT PEER-REVIEWED | Posted: 3 January 2024 doi:10.20944/preprints202401.0163.v1

(2) The low emplacement pressure and the large amount of water in the Nb-Ta-rich melts allow the fractionation of twin pairs (Zr-Hf, Y/Ho and Nb/Ta) together with saturation and exsolution processes of the volatile phase, which are manifested in snowball quartz textures, white mica-rich layers (especially in the margins), aplopegmatites intercalated in the granite (especially in the apical zone), metasomatic processes (albitization), greisen formation and P loss in the feldspars (especially in the plagioclase).

(3) The parental magmas of the Iberian GMRs can be very diverse, mainly two-mica granites and granites with cordierite, although granodiorites and type I granites could be the parental magmas of the P-poor GMRs.

(4) Thermodynamic modeling shows that the high Al and P contents of Nb-Ta rich granites can be explained by melt evolution. This does not occur with the strong Na enrichment of the RMGs and the presence of fluxing elements, albitization or non-equilibrium crystallization processes must be involved.

(5) The samples that best fit the thermodynamic evolution are the aplitic rim facies of the Argemela granite, probably because of their rapid crystallization, which avoided much interaction with the volatile phase and/or fluxing elements.

(6) The absence of inflections in the variation diagrams with Nb and Ta, the high solubility of CGMs in melts rich in fluxing elements, as well as the good fit in two-step models (with major and trace elements) involving white mica, suggest that this mineral played a very relevant role in the evolution of Ta and Ta/Nb in RMGs.

Supplementary Materials: The following supporting information can be downloaded at the website of this paper posted on Preprints.org. Table S1: Mineral chemistry of silicates and CGM from Golpejas granite.

Author Contributions: Conceptualization, F.J.L.-M., A.D.-M. and S.M.T.-S.; methodology, F.J.L.-M., and A.D.-M.; software, F.J.L.-M., and A.D.-M.; validation, F.J.L.-M., A.D.-M. and S.M.T.-S.; investigation, F.J.L.-M.; writing—original draft preparation, F.J.L.-M., A.D.-M, S.M.T.-S and T.L.-G.; writing—review and editing, T.L.-G. and T.S.; visualization, F.J.L.-M.; project administration, A.D.-M. and S.M.T.-S.; funding acquisition, A.D.-M , S.M.T.-S. and T.S.-G. All authors have read and agreed to the published version of the manuscript.

Funding: This research was funded by the European Union Next Generation: Plan de Recuperación, Transformación y Resiliencia, Project C17.i7.CSIC-MET 2021-00-000: Critical Strategic Metals for the Energy Transition (MINECRITICAL). This research has also benefited from the project Forecasting and Assessing Europe's Strategic Raw Materials Needs, FRAME (GeoERA project, grant agreement Nº 731166) and the project MINCE: Study of critical and strategic raw materials for the ecological transition and the supply of the main industrial value chains in Spain, from the Subdirección General de Minas (Ministerio para la Transición Ecológica y el Reto Demográfico).

Acknowledgments: The authors are grateful to the staff of the IGME-CSIC Lithoteque in Peñarroya for providing much of the information used in this publication.

Conflicts of Interest: The authors declare no conflict of interest

References

1. López-Moro, F.J.; Díez-Montes, A.; Llorens-González, T.; Sánchez-García,T.; Timón-Sánchez, S.M. Is the kaolinization process the key to explaining the enrichment of critical metals in the apical zones of rare-metal granites?**.** In Goldschmidt 2023, Lyon, France, 10-07-2023**.**
2. López-Moro, F.J.; García Polonio, F.; Llorens González, T.; Sanz Contreras, J.L.; Fernández Fernández, A.; Moro Benito, M.C. Ta and Sn concentration by muscovite fractionation and degassing in a lens-like granite body: The case study of the Penouta rare-metal albite granite (NW Spain). *Ore Geol. Rev*. **2017**, *82*, 10–30.
3. Llorens, T.; García Polonio, F.; López Moro, F.J.; Fernández, A.; Sanz, J.L.; Moro, M.C. Tin-tantalum-niobium mineralization in the Penouta deposit (NW Spain): Textural features and mineral chemistry to unravel the genesis and evolution of cassiterite and columbite group minerals in a peraluminous system. *Ore Geol. Rev*. **2017**, *81*, 79-95.
4. Alfonso, P., Hamid, S.A., García-Valles, M., Llorens, T., López-Moro, F.J., Tomasa, O., Calvo, D., Guasch, E., Anticoi, H., Oliva, J., Parcerisa, D., García Polonio, F. Textural and mineral-chemistry constraints

Preprints (www.preprints.org) | NOT PEER-REVIEWED | Posted: 3 January 2024 doi:10.20944/preprints202401.0163.v1

regarding the columbite-group minerals in the Penouta deposit: evidences of magmatic and fluid-related processes. *Min. Mag*. **2018**, *82(S1)*, S199-S222.

5. Michaud, J.A.S.; Pichavant, M. Magmatic fractionation and the magmatic-hydrothermal transition in rare metal granites: Evidence from Argemela (Central Portugal). *Geochim. Cosmochim. Acta* **2020**, *289*, 130-157.
6. Wolf, M; Romer, R.L.; Franz, L.; López-Moro, F.J. Tin in granitic melts: The role of melting temperature and protolith composition. *Lithos* **2018**, *310-311*, 20-30.
7. Matte, P. Accretionary history and crustal evolution of the Variscan belt in Western Europe. *Tectonophysics* **1991**, *196*, 309–337.
8. Sánchez Martínez, S.; Arenas, R.; García, F.D.; Martínez-Catalán, J.R.; Gómez-Barreiro, J.; Pearce, J.A. Careón ophiolite, NW Spain: Suprasubduction zone setting for the youngest Rheic Ocean floor. *Geology*, **2007**, *35*, 53–56.
9. Escuder Viruete, J.; Arenas, R.; Martínez-Catalán, J.R. Tectonothermal evolution associated with Variscan crustal extension in the Tormes Gneiss Dome (NW Salamanca, Iberian Massif, Spain). *Tectonophysics* **1994**, *238*, 117-138.
10. Gapais, D.; Lagarde, J.L.; Le Corre, C.; Audren, C.; Jégouzo, P.; Casas Saintz, A.; Van Den Driessche, J. La zone de cisaillement de Quiberon : témoin d'extension de la chaîne varisque en Bretagne méridionale au Carbonifère. *CR Acad Sci II A* **1993**, *316*, 1123–1129.
11. Gapais, D.; Brun, J.P.; Gumiaux, C.; Cagnard, F.; Ruffet, G.; Veslud, CLCD. Extensional tectonics in the Hercynian Armorican belt (France). An overview. *BSGF* **2015**, *186*, 117–129.
12. Matte, P. La chaine varisque parmi les chaines paleozoiques peri atlantiques, modele d'evolution et position des grands blocs continentaux au Permo-Carbonifere. *BSGF* **1986**, *II*, 9–24.
13. Faure, M. Late orogenic carboniferous extensions in the Variscan French Massif Central. *Tectonics* **1995**, *14*, 132–153.
14. Faure, M.; Bé Mézèmé, E.; Duguet, M.; Cartier, C.; Talbot, J.Y. Paleozoic tectonic evolution of medio-europa from the example of the french massif central and massif armoricain. *J Virtual Explor Electron Edit* **2005**, 19, 1–26.
15. Michaud, J.A. Rare metal granites origin, emplacement and mechanisms of the magmatic-hydrothermal transition - Insights from the Argemela Rare Metal Granite (Portugal) and an experimental study. PhD Thesis Univ. D'Orléans, 2019.
16. Chauris, L. Les leucogranites à béryl de Bretagne méridionale. 113e Congrès National des Sociétés Savante, Strasbourg, Sciences de la Terre, 1988, pp. 37-49.
17. Raimbault, L. Composition of complex lepidolite-type granitic pegmatites and of constituent columbite-tantalite, Chedeville, Massif Central, France. *Can. Mineral*. **1998**, *36*, 563–583.
18. Raimbault, L.; Charoy, B.; Cuney, M.; Pollard, P.J. Comparative geochemistry of Ta-bearing granites. In *Source, Transport and Deposition of Metals;* Pagel, M., Leroy, J.L., Eds.; Society for Geology Applied to Mineral Deposits, 1991; pp.793-796.
19. Aubert, G. Les coupoles granitiques de Montebras et d'Échassières:(Massif Central français) et la genèse de leurs minéralisations en étain, lithium, tungstène et béryllium. Éditions BRGM, 1969.
20. Breiter, K.; Durisová, J.; Korbelová, Z.; Lima, A.; Vasinová Galiová, M.; Hlozková, M.; Dosbaba, M. Rock textures and mineral zoning – A clue to understanding rare-metal granite evolution: Argemela stock, Central-Eastern Portugal. *Lithos* **2022**, *410-411*, 106562.
21. Breiter, K.; Mu¨ller, A.; Leichmann, J.; Gabas˘ová, A. Textural and chemical evolution of a fractionated granitic system: the Podlesí stock, Czech Republic. *Lithos* **2005**, *80*, 323–345.
22. Breiter, K.; Ďurišová, J.; Hrstka, T.; Korbelová, Z.; Vaňková, M.H.; Galiová, M.V.; Kanický, V.; Rambousek, P.; Knésl, I.; Dobeš, P.; Dosbaba, M. Assessment of magmatic vs. metasomatic processes in rare-metal granites: a case study of the Cínovec/Zinnwald Sn–W–Li deposit, Central Europe. *Lithos* **2017**, *292*, 198-217.
23. Manning D.A.C.; Hill, P.I. The petrogenetic and metallogenetic significance of topaz granite from the Southwest England orefield. *Geol. S. Am. S.* **1990**, *246*, 51-69.
24. Müller, A.; Seltmann, R.; Halls, C.; Siebel, W.; Dulski, P.; Jeffries, T.; Spratt, J.; Kronz, A. The magmatic evolution of the Land's End pluton, Cornwall, and associated pre-enrichment of metals. *Ore Geol. Revs*. **2006**, *28*, 329-367.
25. Eby, G.N. The A-type granitoids: a review of their occurrence and chemical characteristics and speculations on their petrogenesis. *Lithos* **1990**, *26*, 115–134.

Preprints (www.preprints.org) | NOT PEER-REVIEWED | Posted: 3 January 2024 doi:10.20944/preprints202401.0163.v1

26. Díez-Montes, A.; Martínez Catalán, J.R.; Bellido Mulas, F. Role of the Ollo de Sapo masive felsic volcanism of NW Iberia in the Early Ordovician dynamics of northern Gondwana. *Gondwana Res.* **2010**, *17*, 363-376.
27. Rodríguez-Alonso, M.D.; Peinado, M.; López-Plaza, M.; Franco, P.; Carnicero, A.; Gonzalo, J.C. Neoproterozoic-Cambrian synsedimentary magmatism in the Central Iberian Zone (Spain): geology, petrology and geodynamic significance. *Int. J. Earth Sci.* **2004**, *93*, 897–920.
28. Arenas, R.; Martínez-Catalán, J.R., Díaz García, F. Zona de Galicia-Trás-os-Montes. In *Geología de España*; Vera Torres, J.A., Ed.; Sociedad Geológica de España e Instituto Geológico y Minero de España. pp. 133-165.
29. Dallmeyer, R.D.; Martínez Catalán, J.R.; Arenas, R.; Gil Iberguchi, J.I.; Gutiérrez Alonso, G.; Farias, P.; Bastida, F; Aller, J. Diachronous Variscan tectonothermal activity in the NW Iberian Massif: Evidence from $^{40}Ar/^{39}Ar$ dating of regional fabrics. *Tectonophysics*, **1997**, 277, 307-337.
30. Valverde-Vaquero, P.; Díez-Balda, M.A.; Díez-Montes, A.; Dörr, W.; Escuder-Viruete, J.; González-Clavijo, E.; Maluski, H.; Rodríguez-Fernández, L.R.; Rubio, F.; Villar, P. The ''Hot Orogen'': Two Separate Variscan Low-Pressure Metamorphic Events in the Central Iberian Zone (Abstract 76). Mechanics of Variscan Orogeny: A Modern View on Orogenic Research. Geol France 2. BRGM, 2007.
31. Valle Aguado, B.; Azevedo, M.R.; Schaltegger, U.; Martínez Catalán, J.R.; Nolan, J. U/Pb zircon and monazite geochronology of Variscan magmatism related to synconvergence extension in Central Northern Portugal. *Lithos* **2005**, *82*, 169–184.
32. López-Moro, F.J.; López-Plaza, M.; Romer, R.L. Generation and emplacement of shear-related highly mobile crustal melts: the synkinematic leucogranites from the Variscan Tormes Dome, Western Spain. *Int. J. Earth Sci*. **2012**, *101*, 1273–1298.
33. Gutiérrez-Alonso, G.; Collins, A.S.; Fernández-Suárez, J.; Pastor-Galán, D.; González-Clavijo, E.; Jourdan, F.; Weil, A.B.; Johnston, S.T. Dating of lithospheric buckling: $^{40}At/^{39}Ar$ ages of syn-orocline strike-slip shear zones in northwestern Iberia. *Tectonophysics* **2015**, *643*, 44-54.
34. Arribas, A.; Gonzalo Corral, F.J., Iglesias, M. Génesis de una mineralización asociada a una cúpula granítica: el yacimiento de estaño de Golpejas, (Salamanca). *Cadernos do Laboratorio Xeolóxico de Laxe* **1982**, *3*, 563-592.
35. Chicharro, E. Petrologic-metallogenic characterization of a specialized granite: the Logrosán stock (Cáceres). Ph Thesis, Universidad Complutense de Madrid, Madrid, 2016.
36. Gonzalo Corral, F.J., Gracia Plaza, A.S. Yacimientos de estaño del Oeste de España. *Cadernos do Laboratorio Xeolóxico de Laxe* **1985**, *9*, 265-303.
37. ADARO. Penouta deposit mining research. Volume I. Geological characteristics and reserves. Final Report, 1985, pp. 1-123 (In Spanish).
38. Reginiussen, H.; Jonsson, E.; Hamisi, J.; Timón-Sánchez, S.M.; Díez-Montes, A.; Teran, K.; Salgueiro, R.; Oliveira, D.; Melnik, I. Providing data and intelligence on Nb-Ta mineralizations in Europe to the GeoERA information platform. FRAME WP6, D6.4. 26p. Appendix 1. Analytical data Spanish deposits. 220p, 2021.
39. Solid Mines España. Alberta 5 Golpejas-Salamanca tin-tantalum project. Internal report, 2005.
40. Charoy, B.; Norohna, F. Multistage Growth of a Rare-Element Volatile-Rich Microgranite at Argemela (Portugal). *J. Petrol*. **1996**, *37*, 73-74.
41. Armstrong, E.; Murillo, A.; Pages, J.L. Investigación minera por estaño en la reserva nº 146 "Villardeciervos" (Orense). *Cadernos do Laboratorio Xeolóxico de Laxe* **1983**, *6*, 459-467.
42. ITGE. Estimation of the mining potential in the area of Villardevós (ORENSE). Annex 1, Methodology and content sheets, final report, 1976 (in Spanish).
43. López-Plaza, M.; Rodríguez Alonso, M.D.; Martín Herrero, D.; Albert Colomert, V. Mapa Geológico y Memoria de la Hoja nº 525 (Ciudad Rodrigo), 2ª serie del Mapa Geológico Nacional a escala 1:50.000 (MAGNA). Servicio de Publicaciones IGME, Madrid. 1990, 1-96.
44. Gallego Garrido, M. *Las mineralizaciones de litio asociadas a magmatismo ácido en Extremadura y su encuadre en la zona Centro-Ibérica.* Ph Thesis, Universidad Complutense de Madrid, Madrid, 1992.
45. Garate-Olave, I.; Roda-Robles, E.; Gil-Crespo, P.P.; Pesquera, A.; Errandonea-Martin, J. The Tres Arroyos granitic aplite-pegmatite field (Central Iberian Zone, Spain): petrogenetic constraints from evolution of Nb-Ta-Sn oxides, whole-rock geochemistry and U-Pb geochronology. *Minerals* **2020**, *10*, 1008.
46. IGME (1980). Project: Expansion of the intermediate phase of Sn-W mining research in several areas of Extremadura. El Trasquilón area, final report, 1980, (in Spanish).

Preprints (www.preprints.org) | NOT PEER-REVIEWED | Posted: 3 January 2024 doi:10.20944/preprints202401.0163.v1

47. Chicharro, E.; Martín-Crespo, T.; Gómez-Ortiz, D.; López-García, J.A.; Oyarzun, R.; Villaseca, C. Geology and gravity modeling of the Logrosán Sn–(W) ore deposits (Central Iberian Zone, Spain). *Ore Geol. Rev.* **2015**, *65*, 294–307.
48. ITGE. Basic Study of Tin Deposits. Type-Laza. Memory-annexes and maps, final report, 1976, pp.1-149, (in Spanish).
49. Canosa, F.; Martin-Izard, A.; Fuertes-Fuente, M. Evolved granitic systems as a source of rare-element deposits: The Ponte Segade case (Galicia, NW Spain). *Lithos* **2012**, *153*, 165–176.
50. Gloaguen, E. Apports d'une étude intégrée su les relations entre granites et minéralisations filoniennes (Au et Sn-W) en contexte tardi orogénique (Chaîne Hercynienne, Galice centrale, Espagne). Ph Thesis, University of D'Orleans, 2006.
51. González Aguado, M.T. Mineralizaciones de Sn-Nb-Ta asociadas a cúpulas graníticas de Extremadura. Ph Thesis, Escuela Técnica Superior de Ingenieros de Minas, Madrid, 1985.
52. Merino, E.; Villaseca, C.; Orejana, D.; Jeffries, T. Gahnite, chrysoberyl and beryl co-occurrence as accessory minerals in a highly evolved peraluminous pluton: The Belvís de Monroy leucogranite (Cáceres, Spain). *Lithos* **2013**, *179*, 137-156.
53. ADARO. Research Project for tin and wolfram on the permit "MARIVI" Pedroso de Acim (Cáceres). Volume 1. Final Report, 1984, pp. 1-215 (In Spanish).
54. Ramírez, J.A.; Grundvig, S. Causes of geochemical diversity in peraluminous granitic plutons: the Jálama pluton, Central-Iberian Zone (Spain and Portugal). *Lithos* **2000**, *50*, 171-190.
55. Minera del Duero. Mining work Mina Bellita and Tita (Golpejas): Final report, 1985 (In Spanish).
56. Díez-Montes, A. *La geología del Dominio "Ollo de Sapo" en las comarcas de Sanabria y Terra do Bolo*. Serie NOVA TERRA 34, A Coruña, 2007.
57. Watson, E.B.; Harrison, T.M. Zircon saturation revisited: temperature and compositional effects in a variety of crustal magma types. *Earth Planet. Sci. Lett.* **1983**, *64*, 295–304.
58. Montel, J.M. A model for monazite/melt equilibrium and application to the generation of granitic magmas. *Chem. Geol*. **1993**, *110*, 127–146.
59. Pichavant, M.; Montel, J.M.; Richard, L.R. Apatite solubility in peraluminous liquids: Experimental data and an extension of the Harrison-Watson model. *Geochim. Cosmochim. Acta* **1992**, *56*, 3855-3861.
60. Massonne, H.J.; Schreyer, W. Phengite geobarometry based on the limiting assemblage with k-feldspar, phlogopite, and quartz. *Contrib. Mineral. Petrol*. **1987**, *96*, 212–224.
61. Moore, G.; Vennemann, T.; Carmichael, I.S.E. An empirical model for the solubility of H_2O in magmas to 3 kilobars. *Am. Mineral*. **1998**, *83*, 36–42.
62. Gualda, G.A.R.; Ghiorso, M.S.; Lemons, R.V.; Carley, T. Rhyolite-MELTS: a Modified Calibration of MELTS Optimized for Silica-rich, Fluid-bearing Magmatic Systems. *J. Petrol*. **2012**, *53*, 875-890.
63. Cabero, M.T.; Mecoleta, S.; López-Moro, F.J. OPTIMASBA: a Microsoft Excel workbook to optimise the mass-balance modelling applied to magmatic differentiation processes and subsolidus overprints. *Comput. Geosci*. **2012**, *42*, 206-211.
64. Ersoy, E.Y.; Helvaci, C. FC–AFC–FCA and mixing modeler: A Microsoft® Excel© spreadsheet program for modeling geochemical differentiation of magma by crystal fractionation, crustal assimilation and mixing. *Comput. Geosci*. **2010**, *36*, 383-390.
65. Tischendorf, G.; Gottesmann, B.; Fo¨rster, H.-J.; Trumbull, R.B. On Li-bearing micas: estimating Li from electron microprobe analyses and an improved diagram for graphical representation. *Min. Mag*. **1997**, *61*, 809–834.
66. Van Lichtervelde, M.; Holtz, F.; Melcher, F. The effect of disequilibrium crystallization on Nb-Ta fractionation in pegmatites: Constraints from crystallization experiments of tantalite-tapiolite. *Am. Min*. **2018**, *103*, 1401-1416.
67. London, D. Phosphorus in S-type magmas: The P_2O_5 content of feldspars from peraluminous granites, pegmatites, and rhyolites. *Am. Mineral.* **1992**, *77*, 126-145.
68. London, D.; Morgan VI, G.B.; Babb, H.A.; Loomis, J.L. Behavior and effects of phosphorus in the system Na_2O-K_2O-Al_2O_3-SiO_2-P_2O_5-H_2O at 200 MPa (H_2O). *Contrib. Mineral. Petrol*. **1993**, *113*, 450-465.
69. Linnen, R.L. The effects of water on the solubility of accessory minerals in granitic melts. *Lithos* **2005**, *80*, 267-280.
70. Linnen R.L.; Keppler H. Columbite solubility in granitic melts: Consequences for the enrichment and fractionation of Nb and Ta in the Earth's crust. *Contrib. Mineral. Petrol* **1997**, *128*, 213-227.

Preprints (www.preprints.org) | NOT PEER-REVIEWED | Posted: 3 January 2024 doi:10.20944/preprints202401.0163.v1

71. Linnen R.L.; Cuney, M. Granite-related rare-element deposits and experimental constraints on Ta-Nb-W-Sn-Zr-Hf mineralization. In *Rare-Element Geochemistry and Mineral Deposits;* Linnen, R.L., Samson, I.M., Eds.; Geological Association of Canada, GAC Short Course Notes; 2005, 17, pp. 45-67.
72. Tang, Y.; Zhang, H.; Rao, B. The effect of phosphorus on manganocolumbite and mangaotantalite solubility in peralkaline to peraluminous granitic melts. *Am. Mineral*. **2016**, *101*, 415-422.
73. Frost, B.R.; Frost, C.D.. A geochemical classification for feldspathic igneous rocks. *J. Petrol.* **2008**, *49*, 1955-1969.
74. Frost, B.R.; Barnes, C.G.; Collins, W.J.; Arculus, R.J.; Ellis, D.J.; Frost, C.D. A geochemical classification for granitic rocks. *J. Petrol.* **2001**, *42*, 2033-2048.
75. Pearce. J.A.; Harris, N.B.W.; Tindle. A.G. Trace element discrimination diagrams for the tectonic interpretation of granitic rocks. *J. Petrol.* **1984**, *25*, 956-983.
76. Maniar, P.D.; Piccoli, P.M. Tectonic discrimination of granitoids. *Geol. Soc. Am. Bull*. **1989**, *101*, 635-643.
77. Debon, F.; Le Fort, P. A chemical mineralogical classification of common plutonic rocks and association. *Earth Sci*. **1983**, *73*, 135-149.
78. Villaseca, C.; Barbero, L.; Herreros, V.. A re-examination of the typology of peraluminous granite types in intracontinental orogenic belts. *T. RSE. Earth* **1998**, *89*, 113–119.
79. Le Maitre, R.W.; Bateman, P.; Dudek, A.; Keller, J.; Lameyre, J.; Le Bas, M.J.; Sabine, P.A.; Schmid, R.; Sorensen, H.; Streckeisen, A.; Woolley, A.R.; Zanettin, B. *A classification of igneous rocks and glossary of terms*. Blackwell, Oxford, 1989.
80. Ballouard, C.; Poujol, M.; Boulvais, P.; Branquet, Y.; Tartèse, R.; Vigneresse, J.L. Nb-Ta fractionation in peraluminous granites: A marker of the magmatic-hydrothermal transition. *Geology* **2016**, *44*, 231–234.
81. Förster, H.-J.; Rhede, D. The Be–Ta-rich granite of Seiffen (eastern Erzgebirge, Germany): accessory-mineral chemistry, composition, and age of a late-Variscan Li–F granite of A-type affinity. *N. Jb. Miner. Abh*. **2006**, *182*, 307-321.
82. Bau, M. Controls on the fractionation of isovalent trace elements in magmatic and aqueous systems: evidence from Y/Ho, Zr/Hf, and lanthanide tetrad effect. *Contrib. Mineral. Petrol*. **1996**, *123*, 323–333.
83. Irber, W. The lanthanide tetrad effect and its correlation with K/Rb, Eu/Eu⁄, Sr/Eu, Y/Ho and Zr/Hf of evolving peraluminous granite suits. *Geochim. Cosmochim. Acta* **1999**, *63*, 489–508.
84. Rudnick, R.L.; Fountain, D. Nature and composition of the continental crust: A lower crustal perspective. *Revs. Geophys*. **1995**, *33*, 267–309.
85. Taylor, S.R.; McLennan, S.M. *The continental crust: Its composition and evolution*. Blackwell, Oxford, 1985.
86. Sun, S.S.; McDonough, W.F. Chemical and isotopic systematics of oceanic basalts: Implications for mantle composition and processes. In *Magmatism in ocean basins*, Saunders, A.D., Norry, M.J., Eds.; Geological Society Special Publication. Geological Society, London, 1989; 42, pp. 313–345.
87. González Menéndez, L.; Bea, F. El batolito de Nisa-Alburquerque. In *Geología de España*, Vera, J.A., Ancochea, A., Calvo Sorando, J.P., Barnolas Cortinas, A., Bea Carredo, F., Eds.; SGE-IGME, Madrid, 2004, pp. 120–122.
88. Melleton, J.; Gloaguen, E.; Frei, D.; Lima, A.; Vieira, R.; Martins, T. Polyphased rare-element magmatism during late orogenic evolution: geochronological constraints from NW Variscan Iberia. *B. Soc. Geol. Fr. Earth Sci. B.* **2022**, *193*, 7.
89. Fernández-Suárez, J.; Dunning, G.R.; Jenner, G.A.; Gutiérrez-Alonso, G. Variscan collisional magmatism and deformation in NW Iberia: constraints from U-Pb geochronology of granitoids. *J. Geol. Soc. London*, **2000**, *157*, 565-576.
90. Orejana, D.; Merino, E.; Villaseca, C.; Pérez-Soba, C.; Cuesta, A. Electron microprobe monazite geochronology of granitic intrusions from the Montes de Toledo batholith (central Spain). *Geol. J.* **2012**, *47*, 41–58.
91. Tuttle, O.F.; Bowen, N.L. Origin of granite in the light of experimental studies in the system $NaAlSi_3O_8$-$KAlSi_3O_8$-SiO_2-H_2O. *Geol. Soc. Am. Mem*. **1958**, *74*.
92. Holtz, F.; Pichavant, M.; Barbey, P.; Johannes, W. Effects of H_2O on the liquidus phase relations in the haplogranitic system at 2 and 5 kbar. *Am. Mineral*. **1992**, *77*, 1223-1241.
93. Pichavant, M., Experimental Crystallization of the Beauvoir Granite as a Model for the Evolution of Variscan Rare Metal Magmas. *J. Petrol.* **2023**, *63*, 12 egac120.
94. Mangas, J.; Arribas, A. Fluid inclusion study in different types of tin deposits associated with the Hercynian granites of western Spain. *Chem. Geol.* **1987**, *61*, 193-208.

Preprints (www.preprints.org) | NOT PEER-REVIEWED | Posted: 3 January 2024 doi:10.20944/preprints202401.0163.v1

95. Candela, P.A. A Review of Shallow, Ore-related Granites: Textures, Volatiles, and Ore Metals. *J. Petrol.* **1997**, *38*, 1619-1633
96. Oppenheimer, C.; Fischer, T.P.; Scaillet, B. 4.4.- Volcanic degassing: Process and impact. In *Treatise on Geochemistry*, 2nd ed; Holland, H.D., Turekian, K.K., Eds.; Elsevier, 2014, 4, pp.111-179.
97. Dostal, J.; Kontak, D.J.; Gerel, O.; Shellnutt, J.G.; Fayek, M. Cretaceous ongonites (topaz-bearing albite-rich microleucogranites) from Ongon Khairkhan, Central Mongolia: Products of extreme magmatic fractionation and pervasive metasomatic fluid: rock interaction. *Lithos*. **2015**, *236-237*, 173-189.
98. Fu, J.; Li, G.; Wang, G.; Guo, W.; Dong, S.; Li, Y.; Zhang, H.; Liang, W.; Jiao, Y. Geochemical Evidence for Genesis of Nb-Ta-Be Rare Metal Mineralization in Highly Fractionated Leucogranites at the Lalong Dome, Tethian Himalaya, China. *Minerals* **2023**, *13*, 1456.
99. Tischendorf, G.; Förster, H.-J. Acid magmatism and related metallogenesis in the Erzgebirge. *Geol. J.* **1990**, *25*, 443–454.
100. Ballouard, C.; Couzinié, S.; Bouilhol, P.; Harlaux, M.; Mercadier, M.; Montel, J.M. A felsic meta-igneous source for Li-F-rich peraluminous granites: insights from the Variscan Velay dome (French Massif Central) and implications for rare-metal magmatism. *Contrib. Mineral. Petrol*. **2023**, *178:75*, 1-24
101. Teuscher, E.O. Primäre Bildungen des granitischen Magmas und seiner Restlösungen im Massif von Eibenstock-Neudeck. *Mineralogische und Petrographische Mitteilungen* **1936**, *47*, 211–262.
102. Beus, A.A.; Zhalashkova, N.Y. Postmagmatic high temperature metasomatic processes in granitic rocks. *Int. Geol. Rev.* **1964**, *6*, 668-681.
103. Černý, P.; Blevin, P.L.; Cuney, M.; London, D. Granite-related ore deposits. *Econ Geol* **2005**, *100*, 337–370.
104. Launay, G.; Branquet, Y.; Sizaret, S.; Guillou-Frottier, L.; Gloaguen, E. How greisenization could trigger the formation of large vein-and-greisen Sn-W deposits: a numerical investigation applied to the Panasqueira deposit. *Ore Geol Rev* **2023**, *105299*.
105. Thomas, R.; Webster, J.D. Strong tin enrichment in a pegmatite-forming melt. *Miner. Deposita* **2000**, *35*, 570-582.
106. Romer, R.L.; Kroner, U. Sediment and weathering control on the distribution of Paleozoic magmatic tin-tungsten mineralization. *Miner. Deposita* **2015**, *50*, 327–338.
107. Roda Robles, E.; Villaseca, C.; Pesquera, A.; Gil-Crespo, P.P.; Vieira, R.; Lima, A.; Garate-Olave, I. Petrogenetic relationships between Variscan granitoids and Li-(F-P)-rich aplite-pegmatites in the Central Iberian Zone: Geological and geochemical constraints and implications for other regions from the European Variscides. *Ore Geol. Rev*. **2018**, *95*, 408-430.
108. Manning, D.A.C. The effect of fluorine on liquidus phase relationships in the system Qz-Ab-Or with excess water at 1 Kb. *Contrib. Mineral. Petrol.* **1981**, *76*, 206–215.
109. London, D. 2014. Subsolidus isothermal fractional crystallization. *Am. Mineral*. **2014**, *99*, 543-546.
110. Candela, P.A.; Holland, H.D.. A mass transfer model for copper and molybdenum in magmatic hydrothermal systems: the origin of porphyry-type ore deposits. *Econ. Geol.* **1986**, 81, 1–19.
111. Wang, D.; Liu, J.; Carranza, E.J.M.; Zhai, D.; Wang, Y.; Zhen, S.; Wang, J.; Wang, J.; Liu, Z.; Zhang, F. Formation and evolution of snowball quartz phenocrysts in the Dongping porphyritic granite, Hebei Province, China: Insights from fluid inclusions, cathodoluminescence, trace elements, and crystal size distribution study. *Lithos* **2019**, *340-341*, 239-254.
112. López-Moro, F.J., Díez-Montes, A., Llorens-González, T., Sánchez-García, T., Timón-Sánchez, S.M. Intensive variables in the Golpejas rare metal granite and their implications for ore mineralization. In Reunión Científica de la SEM 2023, Madrid, Spain, 16-06-2023.
113. Raimbault, L.; Burnol, L. The Richemont rhyolite dyke, Massif central, France: A subvolcanic equivalent of rare-metal granites. *Can. Mineral.* **1998**, *36*, 265–282.
114. Linnen R.L. The solubility of Nb-Ta-Zr-Hf-W in granitic melts with Li and Li+F: Constraints for mineralization in rare- metal granites and pegmatites. *Econ. Geol.* **1998**, *93*, 1013-1025
115. Bartels, A.; Holtz, F.; Linnen, R.L. Solubility of manganotantalite and mangano-columbite in pegmatitic melts. *Am. Mineral.* **2010**, *95*, 537–544.
116. Taylor, J.R.P.; Wall, V.J. The behavior of tin in granitoid magmas. *Econ. Geol*. **1992**, *87*, 403–420.
117. Štemprok, M., 1990. Solubility of tin, tungsten and molybdenum oxides in felsic magmas. *Miner. Deposita* **1990**, 25, 205–212.
118. Bhalla, P.; Holtz, F.; Linnen, R.L.; Behrens, H. 2005. Solubility of cassiterite in evolved granitic melts; effect of T, fO_2 and additional volátiles. *Lithos* **2005**, *80*, 387–400.

Preprints (www.preprints.org) | NOT PEER-REVIEWED | Posted: 3 January 2024 doi:10.20944/preprints202401.0163.v1

119. Zaraisky, G.P.; Korzhinskaya, V.; Kotova, N. Experimental studies of Ta_2O_5 and columbite–tantalite solubility in fluoride solutions from 300 to 550°C and 50 to 100MPa. *Miner. Petrol.* **2010**, *99*, 287–300.
120. Nash, W.P.; Crecraft, H.R. Partition coefficients for trace elements in silicic magmas. *Geochimica et Cosmochimica Acta* **1985**, *49*, 2309-2322.
121. López-Moro, F.J., Díez-Montes, A., Llorens-González, T., Sánchez-García, T., Timón-Sánchez, S.M. METALESCRITICOS: a tool for processing geochemical and chemical mineralogical data and obtaining geothermobarometric constraints in granites and rare-metal granites. In Reunión Científica de la SEM 2023, Madrid, Spain, 16-06-2023.

Disclaimer/Publisher's Note: The statements, opinions and data contained in all publications are solely those of the individual author(s) and contributor(s) and not of MDPI and/or the editor(s). MDPI and/or the editor(s) disclaim responsibility for any injury to people or property resulting from any ideas, methods, instructions or products referred to in the content.